

Alma Mater Studiorum – Università di Bologna

DOTTORATO DI RICERCA IN
SCIENZE BIOMEDICHE E NEUROMOTORIE

Ciclo XXXI

Settore Concorsuale: 06/A4

Settore Scientifico Disciplinare: MED/08

**Molecular signatures in thyroid carcinoma and in its potential
precursor lesions**

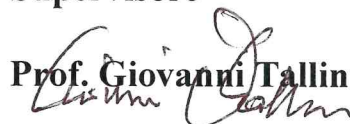
Presentata da: Giorgia Acquaviva

Coordinatore Dottorato

Prof. Pietro Cortelli

Supervisore

Prof. Giovanni Tallini



Esame finale anno 2019

Abstract

Introduction. *BRAF* exon 15 mutations are the most common molecular alterations found in Papillary Thyroid Carcinoma (PTC). The molecular profile of PTC has been thoroughly investigated. However, to date, there is no information regarding the *BRAF* molecular profile of the non-neoplastic tissue surrounding PTCs. Exploring the molecular signature of non-malignant tissue may help to better understand thyroid tumorigenesis and the events that lead potential precursor lesions to evolve towards carcinoma. It has long been speculated that some thyroid nodules may eventually progress to thyroid carcinoma. Although the molecular profile of these nodules with the potential to progress to carcinoma is still undefined, pre-operative molecular analysis helps to identify those nodules that are neoplastic, with either a *RAS-like* (TCGA 2014) or a *BRAF-like* (TCGA 2014) profile, and that need therefore to be excised. The definition of molecular panels can be very useful to inform treatment, to identify the best surgical approach in case excision of the nodule is necessary, and to stratify patient risk in case a malignant diagnosis (carcinoma) is established by histologic examination.

Aim 1 of this project is to establish whether *BRAF* mutations are present in non-malignant tissue surrounding PTC, and in case they are found to characterize their activity in vitro.

Aim 2 of this project is to set up a RNA based expression panel that may provide diagnostic, predictive and prognostic information on thyroid nodules/neoplasms.

Material and Methods. *Aim 1:* we screened the *BRAF* exon 15 molecular status in 30 PTCs and in 100 samples of non-malignant tissue surrounding the tumor, using a Next Generation Sequencing platform. *BRAF* mutations were identified (see Results). Therefore, expression vectors for the BRAF-G593D, BRAF-A598T, BRAF-S607F and BRAF-S607P mutants were

generated. Their kinase activity was evaluated measuring the activation of the MAPK pathway. This activity was then compared to that of BRAF-WT, BRAF-V600E and BRAF-K601E proteins.

Aim 2: we designed a RNA-based expression panel to detect fusion and to identify dysregulated expression of genes known to be altered in thyroid cancer, and with the potential for diagnostic and clinical relevance. We analyzed a set of 44 fresh-frozen (FF) samples. Forty-one FF specimens included normal thyroid tissue, non-malignant tissue (Hyperplasia and Follicular adenoma) and the most common types of thyroid carcinoma: PTC-classical variant, PTC-tall cell variant, PTC-follicular variant, Follicular thyroid carcinoma, Hürthle cell carcinoma, Anaplastic thyroid carcinoma and Medullary thyroid carcinoma. Three specimens of Colorectal cancer were analyzed as gene expression controls.

Results. *Aim 1:* ten of 30 (33.3%) PTC analyzed were BRAF-WT, while 20 were *BRAF*-positive (66.6%). In 9 of 100 samples (9.0%) of non-malignant tissue surrounding the PTC we identified “uncommon” *BRAF* mutations, including p.G593D, p.A598T, p.S607F and p.S607P. The kinase activity of BRAF-G593D, BRAF-A598T, BRAF-S607F and BRAF-S607P were evaluated: BRAF-S607F and BRAF-S607P had the same kinase activity of the BRAF-WT protein; the BRAF-A598T and BRAF-G593D proteins showed decreased kinase activity. All “uncommon” *BRAF* mutations had a lower kinase activity if compared to BRAF-V600E or BRAF-K601E.

Aim 2: the samples with the *BRAF* p.V600E mutation had dysregulated expression of those genes that characterize the BRAF-like molecular profile present in our RNA based panel. Similarly, the samples with RAS mutations had dysregulated expression of those genes that characterize the RAS-like profile present in our panel. Samples with *BRAF* p.V600E had overexpression of our panel genes with a role in cell proliferation. Unsupervised hierarchical analysis of the expression profile identified three major clusters in our samples: i) non-malignant tissue; ii) malignant tissue; iii) non-follicular thyroid cell derived cancers.

Conclusion. *Aim 1:* non-malignant tissue surrounding the thyroid tumor may harbor “uncommon” *BRAF* mutations. However, these mutations do

not significantly affect the kinase activity of the altered BRAF protein. Our findings indicate that BRAF mutations happen randomly in thyroid follicular cells. These “uncommon” BRAF mutants however, do not possess the tumorigenic potential necessary for the development of PTC.

Aim 2: our panel was designed to detect fusion and to identify dysregulated expression of genes known to be altered in thyroid cancer. We show that the panel identifies three main profiles corresponding to: i) non-malignant tissue; ii) malignant tissue; iii) non-follicular thyroid cell derived cancers. This novel RNA based panel may be very useful to complement the preoperative evaluation of thyroid nodules.

Summary

Introduction	1
1 The thyroid gland	1
1.1 Embryology and anatomy	1
1.2 Physiology	1
2 Thyroid neoplasia.....	3
2.1 Benign and Borderline Neoplasm.....	4
2.2 Papillary Thyroid Carcinoma (PTC).....	4
3.3 Follicular Thyroid Carcinoma (FTC).....	6
3.4 Oncocytic (Hürthle cell) Carcinoma	7
2.5 Poorly-Differentiated Thyroid Carcinoma (PDTC)	7
2.6 Anaplastic Thyroid Carcinoma (ATC).....	8
3 Principal molecular alterations in follicular cell-derived neoplasm	8
3.1 TSH receptor/cAMP pathway	9
3.2 Mitogen-activated protein kinase pathway	11
3.2.1 Tyrosine Kinase Receptors.....	12
3.2.1.1 RET	13
3.2.1.2 NTRK	14
3.2.1.3 ALK	16
3.2.2 BRAF.....	17
3.2.3 RAS	19
3.3 PI3K/PTEN/AKT pathway	20
3.4 PPAR γ rearrangement.....	22
Aims of the study	27
Material and Methods	28
1 Next Generation Sequencing.....	28
1.1 Cases selection	28
1.2 Detection of BRAF mutations	29
1.2.1 DNA extraction and quantification.....	29
1.2.2 Amplicon library preparation	29

1.2.3	Library purification and quantification	31
1.2.4	Amplicons dilution, pooling and EmulsionPCR	31
1.2.5	Recovery and enrichment.....	32
2	Site-direct mutagenesis and cell trasfection	33
2.1	Mutant BRAF plasmids generation via site-directed mutagenesis	33
2.2	Cell transfection	35
3	Western blot.....	35
4	Gene panel design	37
5	Selection of cases	38
6	Next Generation Sequencing.....	39
6.1	DNA and RNA extraction.....	39
6.2	Retrotranscription and Next Generation Sequencing Protocol.....	39
7	Statistical analysis	41
	Results	42
1	Next Generation Sequencing.....	42
1.1	Thyroid neoplasia molecular profile	42
1.2	Non-malignant thyroid tissue molecular profile	42
2	Functional characterization of <i>BRAF</i> mutations	48
2.1	Selection of mutant to test.....	48
2.2	Functional characterization	49
3	Gene panel results.....	51
	Discussion	54
	References	59
	Supplementary table	69

Abbreviation

ATY: atypia

ATC: anaplastic thyroid carcinoma

CNS: central nervous system

CRC: colorectal cancer

EFVPTC: noninvasive encapsulated follicular variant of papillary thyroid carcinoma

FA: follicular adenoma

FA-ONC: oncocytic follicular adenoma

FF: fresh-frozen

FFPE: formalin-fixed paraffin-embedded

FNA: fine-needle aspiration

FTC: follicular thyroid carcinoma

HYP: hyperplasia

HTA: hyperfunctioning thyroid carcinoma

MAPK: mitogen-activated protein kinase

MAPKKK: mitogen-activated protein kinase kinase kinase

MIT: mono-iodotyrosine

MOC: malignant oncocytic carcinoma

MTC: medullary thyroid carcinoma

NIFTP: noninvasive follicular thyroid neoplasm with papillary-like nuclear features

NORM: normal tissue

NSCLC: non-small cell lung carcinoma

PDTC: poorly-differentiated thyroid carcinoma

PTC: papillary thyroid carcinoma

PTC-CL: papillary thyroid carcinoma classical variant

PTC-FV: papillary thyroid carcinoma follicular variant

PTC-TC: papillary thyroid carcinoma tall cell variant

PsB: psammoma body

RTK: receptor tyrosine kinase

TSH: thyroid-stimulating hormone

TSHR: TSH receptor

WDT-UMP: well-differentiated tumor of uncertain malignant potential

WDTC: well-differentiated thyroid carcinoma

Introduction

1 THE THYROID GLAND

1.1 EMBRYOLOGY AND ANATOMY

The word for the thyroid gland derives from the Greek *thyreoeidos*, with the meaning of “shield gland” (*thyreos* – shield; *eidos* – form). It is the first endocrine organ that develops from the endoderm during the third week of gestation until the eleventh week. The thyroid originates from *foramen cecum*, an invagination in the floor of the pharynx, that undergoes enlargement, difurcation, lobulation and detachment from the pharynx. Its development results in a butterfly-shaped gland located at the base of the neck, and it consists of two *lateral lobes* united by the *isthmus*, a thin band of connective tissue (**Figure 1.A**).

In a healthy adult, a normal thyroid gland weighs 15-25 g, and each lobe is about 4 cm in length and 15-20 mm in width, with a thickness of 20-39 mm. It is important to notice that these parameters are very variable, especially they could be altered due to any disease.

The gland’s principal histological architecture is the *follicle*, a single layer of epithelial cells, called thyroid *follicular cells*, which is filled with *colloid* (**Figure 1.B**). In between the follicles another subtype of cells, named *parafollicular cells* or *C cells*, are seen.

The follicular cells are responsible for iodine uptake and L-triiodothyronine (T3) and L-thyroxine (T4) synthesis, while C cells are designated for the secretion of calcitonin, involved in calcium homeostasis (**Figure 1.B**). [1, 2]

1.2 PHYSIOLOGY

The thyroid hormones synthesis is under the control of hypothalamic-pituitary axis by negative feedback. The hypothalamus secretes the thyrotropin-releasing hormone (TRH), which stimulates the release from the anterior pituitary gland of thyroid-stimulating hormone (TSH). When the

gland receives TSH stimulation, it starts to synthesize hormones, through a complex process. First, the iodide (I^-) is actively uptaken in exchange for Na^+ , involving ATPase-dependent transport. I^- requires to be organified and incorporated into a tyrosine residue within thyroglobulin: this process is catalyzed by the heme-containing enzyme thyroid peroxidase (TPO) and takes place in the apical membrane of the follicular cell. Once iodinated, thyroglobulin is taken up into the colloid where a coupling reaction between pairs of iodinated tyrosine molecules occurs. The coupling of two tyrosine residues each iodinated at two positions (di-iodotyrosine, DIT) produces T4, whilst the combination of DIT with mono-iodotyrosine (MIT) produces T3. This coupling is catalyzed by TPO.

Thyroid hormones are lipid soluble molecules released only after TSH stimulation, otherwise they are stored in the colloid. When TSH binds its receptor, the G proteins associated with the I loops is activated. There are two different G proteins coupled to the TSH receptor, G_s and G_q , and they stimulate adenylate cyclase and phospholipase C, respectively. The activation of further signal transduction mechanisms stimulate several processes involved in thyroid hormone synthesis and release and thyroid growth, including iodine uptake, production of hydrogen peroxide and TPO and uptake of colloid droplets.

The thyroid hormones bind to nuclear receptor, with a preferential affinity for T_3 , and they regulate gene expression in target cells. In most tissues (excluding brain, spleen and testis) thyroid hormones stimulate the metabolic rate by increasing the number and size of mitochondria, stimulating the synthesis of enzymes in the respiratory chain and increasing membrane $Na^+ -K^+$ ATPase concentration and membrane Na^+ and K^+ permeability [1-3].

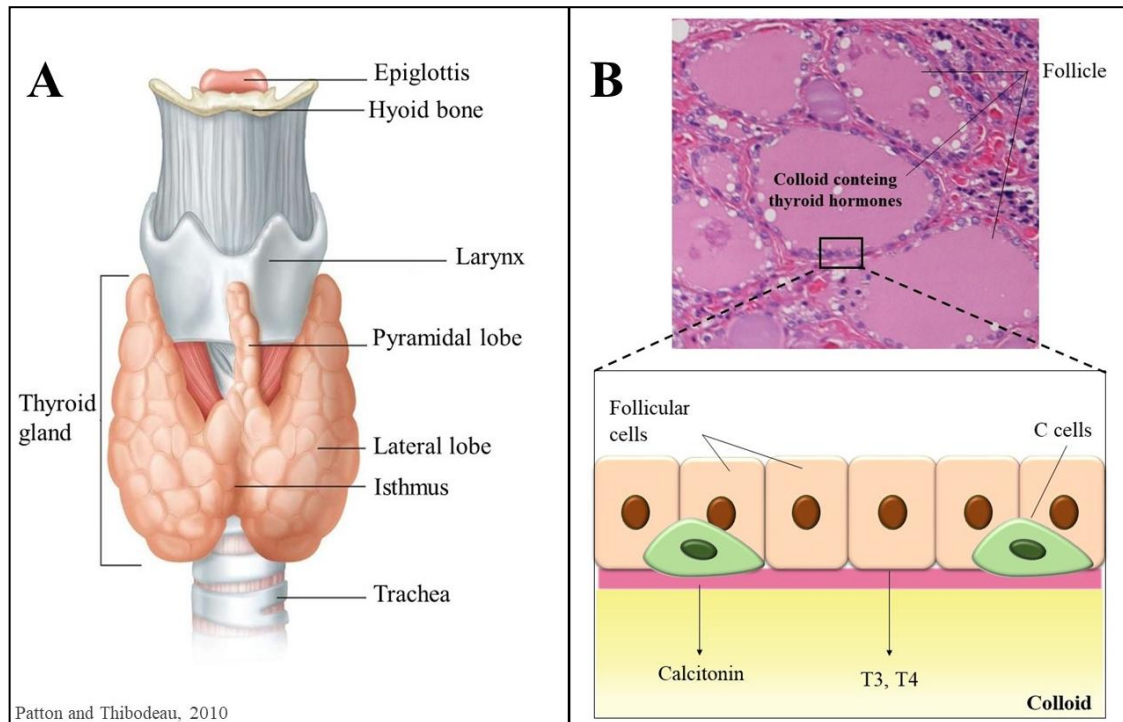


Figure 1: A) Anatomy of thyroid gland; B) Histological architecture of a thyroid gland. The follicles are the functional unit of the gland. They are a roughly spherical group of cells surrounding a central lumen filled with a protein-rich storage material, the colloid. The size of the follicles varies significantly and they range in size 50-500 μm . T3: L-triiodothyronine; T4: L-thyroxine

2 THYROID NEOPLASIA

Thyroid cancer is the most common malignancy of endocrine system [4], and its incidence rates have rapidly increased over the past years, due to earlier detection of small asymptomatic cancers [4, 5].

The vast majority (~95-97%) of thyroid neoplasms, both malignant and benign, arise from follicular cells (**Figure 2**). Thyroid cancers are divided into well-differentiated thyroid carcinomas (WDTCs) (which include both papillary thyroid carcinoma - PTC - and follicular thyroid carcinoma - FTC), poorly differentiated thyroid carcinoma (PDTC), and anaplastic thyroid carcinoma (ATC). PTC and FTC typically respond to radioactive iodine treatment, while PDTC and ATC have a more aggressive behavior [6]. A small percentage (~3-5%) of cancers are classified as medullary

thyroid carcinomas (MTC) (**Figure 2**) and arise from parafollicular C cells [7].

In this thesis, we had focused our attention on follicular cell-derived neoplasm.

2.1 BENIGN AND BORDERLINE NEOPLASM

Benign or borderline thyroid lesions comprise some neoplasm that do not show any invasive or aggressive behavior.

Follicular adenoma (FA) is a benign neoplasm that arises from follicular cell and it is characterized by the presence of glandular structures. FA is usually an encapsulated tumor in which the most common architectural features are follicular or trabecular. FA could be considered as a precursor for some FTC: in fact, they are distinguished histologically only by the presence of capsular and/or vascular invasion, and nowadays there is not any molecular test to reliably discriminate between FA and FTC [8].

Hyperfunctioning thyroid adenoma (HTA), also called toxic adenoma, or Plummer adenoma, is a follicular adenoma that is scintigraphically ‘hot’ and sometimes associated with overt hyperthyroidism.

Well-differentiated tumor of uncertain malignant potential (WDT-UMP) is a follicular neoplasm with both equivocal nuclear features of PTC and capsular/vascular invasion. The vast majority of WDT-UMPs show an indolent behavior [9].

Noninvasive follicular thyroid neoplasm with papillary-like nuclear features (NIFTP) is a non-invasive neoplasm with follicular-growth pattern nuclear features of PTC. It was previously known as *noninvasive encapsulated follicular variant of papillary thyroid carcinoma* (EFVPTC) [10].

2.2 PAPILLARY THYROID CARCINOMA (PTC)

PTCs represent 85–90% of thyroid cancers [11, 12] (**Figure 2**). They usually are diagnosed with fine-needle aspiration (FNA) when they presents

as painless nodule in neck or cervical node. The invasion of parathyroid gland may occur early [13].

PTCs show usually a favorable outcome, but 10–15% patients have recurrent or persistent disease [10, 12]. In a small percentage (~5%) PTC develops distant metastases, especially in lung, bones and central nervous system (CNS) [12]. Some different risk factors are known to be involved in PTC development such as lymphocytic thyroiditis (e.i. Hashimoto thyroiditis) [14], reduced iodine intake, family history and hormonal factor. Radiation exposure is an important risk factor with PTC: it has been demonstrated an association between its development and radiation exposure as a consequence of nuclear fallout after the atomic bombs of Hiroshima and Nagasaki, nuclear testing in the Marshall and Nevada, and the nuclear accident in Chernobyl or Fukushima [15-18].

PTC occurs in about 4.5% of cases as a familial disease, but shows the same prognosis as the sporadic one [19].

Based on the clinical, pathological, histological and molecular profile, according to WHO (World Health Organization) classification PTC could be divided in 15 variants, on the basis of size (papillary microcarcinoma), growth pattern (follicular, macrofollicular, cribriform-morular, and solid), or cellular characteristics (tall cell, hobnail/micropapillary, columnar cell, and oncocyctic) [10]. Histologically, it is possible to observed *psammoma bodies* (PsB), that are considered to be due to tumor cell necrosis.

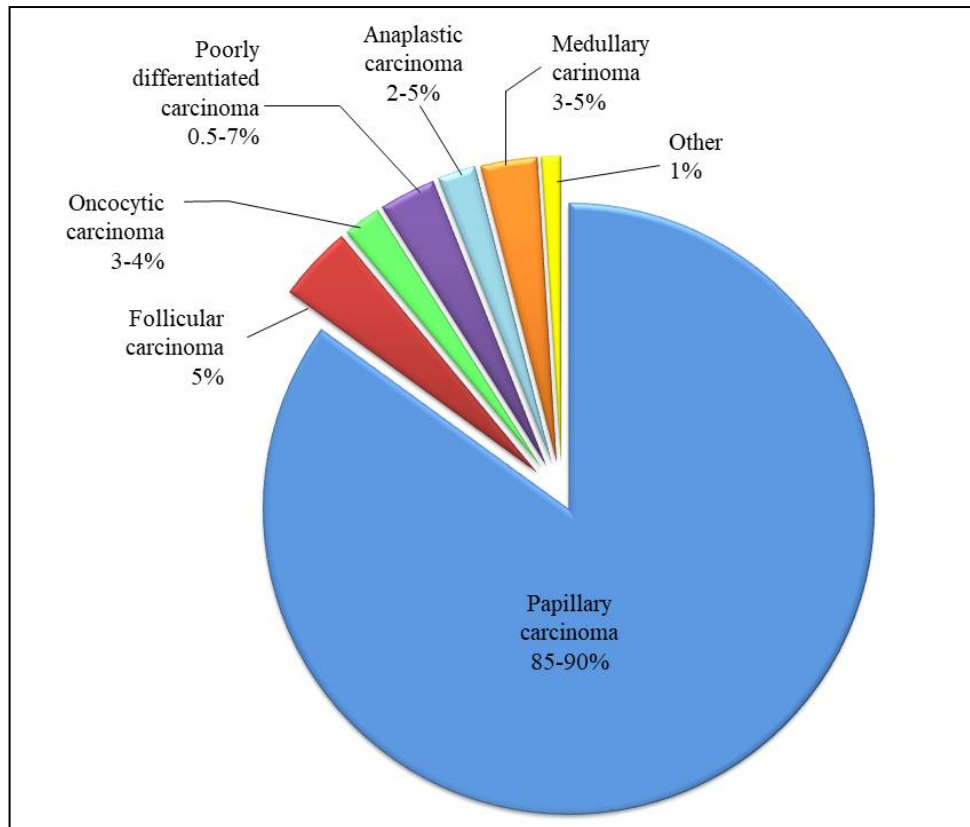


Figure 2: Frequency of the main histological types of thyroid cancer.

2.3 FOLLICULAR THYROID CARCINOMA (FTC)

FTCs are a group of epithelial tumor, showing follicular differentiation but no papillary nuclear features. They represent ~5% of all thyroid malignancies (**Figure 2**), and are known to have a common tumorigenic pathway with FAs, different from that of PTCs (**Figure 3**) [20] [21].

FTC shows a more aggressive behavior than PTC, and tends to spread to distant sites and to metastasize to lymph nodes [22]. Nevertheless, the prognosis is similar in age-matched and disease stage-matched patients [23].

According to the WHO Classification [10], they could be subdivided in three main different types:

- i) *minimal invasive follicular carcinoma*, characterized by capsular invasion only;

- ii) *encapsulated angioinvasive follicular carcinoma*, that represents a type of cancer with limited vascular invasion. It usually shows a better prognosis than those with extensive vascular invasion;
- iii) *widely invasive follicular carcinoma*, which shows an extensive invasion of thyroid and extrathyroidal soft tissues.

2.4 ONCOCYTIC (HÜRTHLE CELL) CARCINOMA

Oncocytic (Hürthle cell) carcinomas represent a rare group (~3–4%) of follicular neoplasm [24] (**Figure 2**), characterized by >75% oncocytic cells content. They show a very distinctive granular cytoplasmic eosinophilia, due to the aberrant increase in mitochondrial mass [25]. The oncocytic tumor is usually encapsulated. If there is not any invasion, they are diagnosed as “benign oncocytic adenomas”, with no recurrence after their excision. On the contrary, they are considered as “malignant oncocytic thyroid carcinomas” (OTCs) when they are invasive and show an aggressive behavior, with higher frequency of extrathyroidal extension, local recurrence and metastasis to lymph nodes [25].

Oncocytic thyroid tumors were traditionally considered subtypes of FA or FTC, and less frequently of PTC. However, recently, they become a separate entity and in WHO classification they are no more considered as a subtype of FA or FTC [10].

2.5 POORLY-DIFFERENTIATED THYROID CARCINOMA (PDTC)

PDTC is a malignant follicular cell-derived tumor that shows a limited differentiation of follicular cell, with a clinical behavior intermediated between WDTC and ATC [10, 26, 27]. While some PDTCs arise *de novo*, some of them are due to de-differentiation of FTC or PTC. They represent 0.5-7% of thyroid malignancies [28, 29] (**Figure 2**), with no evidence of the association between PDTC and radiation exposure [30], while a reduce iodine intake may be a risk factor in its development.

Clinically, PDTC has a more aggressive behavior than WDTC, with a worse prognosis than PTC or FTC. PDTC frequently shows vascular invasion (60-90% cases) and extension to perithyroidal soft tissue in 60-70% cases; distant metastasis are common, especially in lung and bone [27].

2.6 ANAPLASTIC THYROID CARCINOMA (ATC)

ATCs are aggressive undifferentiated (high grade) carcinoma. Nevertheless they represent only the 2 - 5% of all thyroid cancers, ATCs are responsible of 40% of deaths from thyroid cancer [10] (**Figure 2**). ATC often affects old patients, with a mean age at diagnosis of ~71 years [31].

ATC can develop from more differentiated tumors as a result of dedifferentiating steps including the loss of p53 [32], or arises *de novo*. One of the most frequent risk factor is iodine deficiency, and a history of goiter was shown to be associated in 80% of patients with ATC [33-35].

ATCs often present with local invasion and distant metastases, especially in lungs and pleura, brain and bones. A few case have metastases to the skin, liver, kidneys, pancreas, heart, and adrenal glands.

3 PRINCIPAL MOLECULAR ALTERATIONS IN FOLLICULAR CELL-DERIVED NEOPLASM

According to an increased knowledge of the genetic pathology of thyroid tumors, it is now more clear the association between histological features (phenotype) and molecular alterations (genotype) [36]. Moreover, it could indicated that different genetic alterations may be associated with specific stages in a multistep tumorigenic process (**Figure 3**).

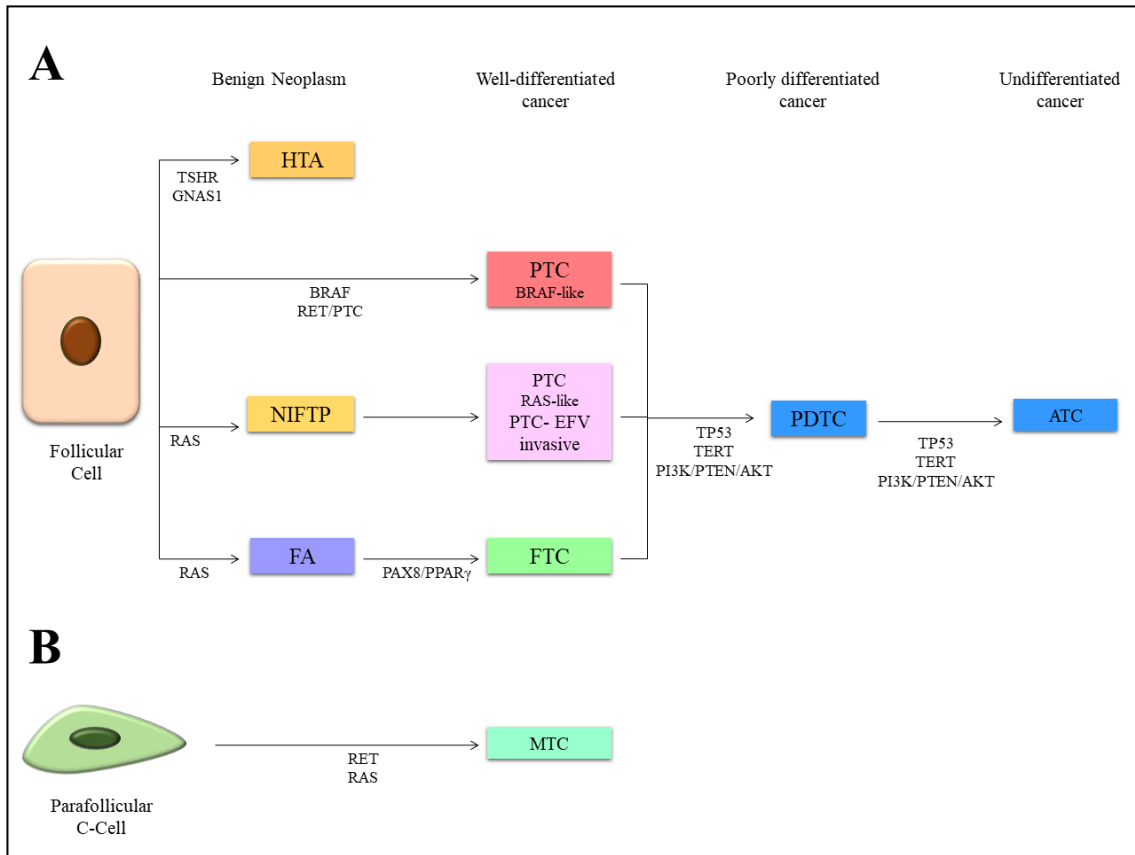


Figure 3: Tumorigenesis in the thyroid gland. [37]

Many different molecular signaling pathways are considered to be involved in the development of thyroid cancer, such as TSH receptor/cAMP pathway, mitogen-activated protein kinase (MAPK) pathway, and PI3K/PTEN/AKT pathway.

3.1 TSH RECEPTOR/CAMP PATHWAY

The thyroid-stimulating hormone receptor (TSHR) is linked to a G protein and, as all the other member of the G protein-coupled receptor member, it presents the characteristic seven loops transmembrane domain [38]. Cyclic adenosine monophosphate (cAMP) plays a crucial role in the TSH-mediated cellular response (**Figure 4**). When TSH binds its receptor, an intracytoplasmic conformational change takes place, resulting in the dissociation of the G α subunit from the G protein complex. G α subunit

can interact with two main proteins: adenylate-cyclase and phospholipase C. The binding of G α to adenylate cyclase produces cAMP, which activates cAMP-dependent protein kinase A (PKA) catalyzing the phosphorylation of specific serine/threonine residues of selected proteins. The cAMP, through the interaction with RAS-associated protein 1 (RAP1), can activate BRAF and, consequently, the MAPK pathway.

Mutations in *TSHR* or in *GNAS* (encoding its associated alpha-subunit of the stimulatory guanine nucleotide-binding protein - G α) genes constitutively activate their protein, with stimulation of the cAMP pathway independent from the binding of TSH to its receptor. The increased intracellular cAMP levels result in the continuous thyroid hormone synthesis and secretion.

The *GNAS* gene can be considered as oncogene and it was first described to be involved in endocrine neoplasms in 1990 [39]. It is located on the long arm of chromosome 20 in humans and encodes multiple gene proteins, including G α . Most of the molecular alterations occur in the mutational hotspot in codons 201 and 227 [39, 40], encoding the GTP-binding domain and resulting in a constitutively active GTP-bound protein form [41].

TSHR is located in on the long arm of chromosome 14 and encodes for a seven-(pass)-transmembrane domain receptors. In 1993, mutations of the *TSHR* gene were first reported [42]: high concentration of genetic alterations in the III intracellular loop and VI transmembrane region, both of which involved in the interaction with G proteins, were observed [43]. The III intracellular loop and VI transmembrane regions This areas correspond mainly to exon 10 of *TSHR* gene, that is usually analyzed [41]. Some germline mutations in *TSHR* are involved to non-autoimmune autosomal dominant hyperthyroidism [44].

TSHR or *GNAS* activating mutations are often observed in follicular adenomas and hyperplastic thyroid nodules, in association with hyperthyroidism, and have been rarely reported in carcinoma [41].

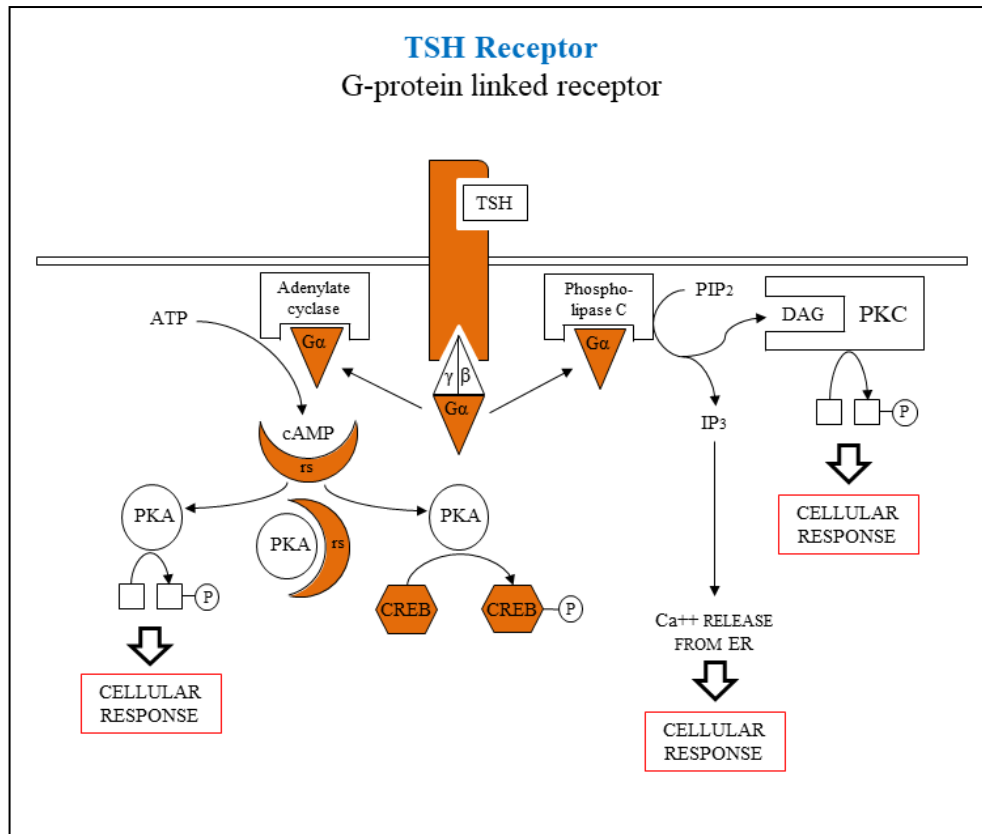


Figure 4: Main molecules altered in thyroid neoplasms (in orange) involving G-protein linked receptor.

TSH: thyroid-stimulating hormone; ATP: adenosine-5'-triphosphate; cAMP: cyclic adenosine monophosphate; G α : G α subunit of heterotrimeric G proteins; β : β subunit of heterotrimeric G proteins; γ : γ subunit of heterotrimeric G proteins; rs: regulatory subunit type 1-a of protein kinase A (encoded by PRKAR1A); PKA: protein kinase A; CREB: cAMP response element-binding protein (CREB3L2 a CREB3 related protein is rearranged with PPAR γ in a few follicular carcinomas); PIP $_n$: phosphatidylinositol n-phosphate; IP $_3$: inositol triphosphate; DAG: diacylglycerol; PKC: protein kinase C.

3.2 MITOGEN-ACTIVATED PROTEIN KINASE PATHWAY

The mitogen-activated protein kinases (MAPKs) belong to a highly conserved family of protein involved in the regulation of many physiological processes in mammalian, including cell proliferation and differentiation, development, immune function, stress responses and cell death (**Figure 5**).

When the ligand binds the receptor tyrosine kinase RTK, this event causes the dimerization of RTK and the phosphorylation of cytoplasmic domains. Cytoplasmic adaptor proteins binds RTK and in turn attract guanine-

nucleotide exchange factors (GEFs) to the plasma membrane. GEFs activate RAS, GTPase protein that becomes transiently active when GEF displaces GDP from RAF and allows GTP to bind; RAS then cleaves the bound GTP and becomes inactive again. During the time it is active, RAS triggers a protein kinase known generally as a mitogen-activated protein kinase kinase kinase (MAPKKK). The MAPKKK protein is BRAF, which facilitates phosphorylation of the second protein kinase in the cascade, MAPKK (MEK) [45].

MAPK pathway consists of a core three-component kinase cascade or module; MAPKs are activated by the phosphorylation of serine/threonine-specific residues within signature T-X-Y motif catalyzed by a dual specific MAPK kinase (MKK or MEK). Downstream the cascade there are many different substrate and effector, such as the p42/p44 MAPKs or extracellular signal regulated kinases (ERKs), the Jun N-terminal kinases (JNKs 1–3), and the p38 MAPKs (α , β , γ , and δ) [46-48].

The constitutive activation of the MAPK pathway is one of the most frequent oncogenic events in many human cancers, and in thyroid tumorigenesis as well. Pathogenic alterations in MAPK cascade is reported in approximately 70% of WDTC, and they can affect tyrosine kinase receptor proteins (RET, NTRK1, ALK, MET) or intracellular downstream effectors like RAS and BRAF [20, 21, 49]. Rarely different molecular mutations in MAPK cascade coexist in the same tumor and this evidence suggests that constitutive activation of only one component of the cascade is sufficient to promote tumor growth [20, 21, 49].

3.2.1 Tyrosine Kinase Receptors (RET, NTRK1, NTRK3, ALK)

Tyrosine kinase receptors are fundamental for signal transduction in many pathway, and they are found to have an altered activity in many cancers. In thyroid neoplasia, more than 20 tyrosine kinase receptors are reported to be involved in tumorigenesis [50]; among these, RET, NTRK1, NTRK3 and ALK are the most important.

3.2.1.1 *RET (rearranged during transfection)*

RET gene is located on the long arm of chromosome 10 (10q11.21) and encodes a transmembrane tyrosine-kinase receptor. Three different *RET* isoforms are known, due to an alternative splicing in region 3' [51]. *RET* receptor consists in a glycosylated extracellular (EC) domain involved in the recognition and binding ligands and co-receptors, a single pass transmembrane (TM) domain, a juxtamembrane (JM) domain, and two intracellular tyrosine kinase domains (TK1 and TK2) required for autophosphorylation [52]. A protein complex which includes *RET*, its ligand, and a GFR α co-receptor (**Figure 5**) is required for the dimerization of *RET* and the activation of downstream signaling, including the RAS-MAPK kinase and the PI3K/PTEN/AKT pathways [53].

RET is expressed in many tissue, such as brain, thymus, testis, and cells of postulated neural crest origin, including calcitonin-producing thyroid C-cells, and a variety of neuroendocrine tissues. On the contrary, it is not expressed in normal follicular cells [54].

Some gain of function (GOF) germline *RET* point mutations are known to be responsible of multiple endocrine neoplasia (MEN) type 2 (MEN 2A, MEN 2B) and familial medullary thyroid carcinoma (fMTC) [55, 56]. Because of GOF mutations frequently occur in the extracellular cysteine-rich domain or in intracellular tyrosine kinase domain, exons 10, 11, 13, 14, 15, and 16 are suggested to be screened in patients with suspected fMTC or MEN2 [57]. *RET* mutations are also reported in sporadic MTC in 30-70% of cases, in association with aggressive behavior and poor prognosis [57-59].

RET is found to be altered in PTC by chromosomal rearrangements that create the *RET/PTC* (because is typically found in papillary thyroid carcinoma) oncogenes [60]. *RET/PTC* rearrangement involves the intron 11 of *RET* and it can be a paracentric inversions or an interchromosomal translocation. The result of these rearrangements is the fusion of the distal part of *RET*, including the region encoding the tyrosine-kinase domain, with heterologous genes that consequently causes an aberrant expression of *RET* in thyroid follicular cells, where it is not normally expressed [60]. More

than twenty heterologous genes have been found fused to *RET* [18, 61-70], usually in thyroid tumors of young patients and children, and in tumors that show a classic papillary histology [71]. Rearrangements of *RET* were initially numbered from 1 to 7; the ~90% of all these chromosomal alterations that occur in PTC are *RET/PTC1* (*RET* fusion with *CCD6*; coiled-coil domain containing 6 gene) and *RET/PTC3* (*RET* fusion with *NCOA4*, nuclear coactivator 4 gene) [72]. The third most frequent rearrangement is *RET/PTC2* (*RET* is fused with *PRKARIA* (protein kinase cAMP-dependent type I regulatory subunit α).

After the Chernobyl disaster (1986), a high incidence of *RET* rearrangements were found in PTC, especially in children. That is the main evidence of the association of *RET/PTC* with radiation exposure, both therapeutic and environmental [16, 73, 74].

3.2.1.2 *NTRK* (neurotrophic receptor tyrosine kinase)

The NTRK family includes three transmembrane tyrosine kinases receptors, NTRK1, NTRK2 and NTRK3 (also known as TRKA, TRKB, TRKC), encoded by the *NTRK1*, *NTRK2* and *NTRK3* genes, respectively. They are mainly expressed in human neuronal tissues and play crucial roles in the development and function of the nervous system through activation by neurotrophins (NTs)[75]. All NTRK receptors are structured with an extracellular domain for ligand binding, a transmembrane region and an intracellular domain with a kinase domain. When the ligand binds the receptor, it triggers the dimerization of the receptors and phosphorylation of specific tyrosine residues in the intracytoplasmic kinase domain. This event results into the activation of downstream, including the RAS-MAPK kinase and the PI3K/PTEN/AKT pathways (**Figure 5**) [75].

NTRK family is known to be involved in cancer development since 1986 [76], and *NTRK1* and *NTRK3* play an important role in thyroid tumorigenesis.

The *NTRK1*, located on the long arm of chromosome 1 (1q23.1), encodes a protein which binds the nerve growth factor (NGF) with high affinity. Similar to RET receptor, the NTRK1 is not present in normal follicular

cells, but it is expressed when the tyrosine kinase domain of *NTRK1* is fused to the 5'-terminal region of heterologous genes. Consequently, these chromosomal rearrangements drive NTRK1 expression in thyroid follicular cells. The resulting chimeric products exhibit constitutively active tyrosine kinase activity [77-80].

Seven heterologous genes have been found fused to *NTRK1* [63, 68, 81, 82], but among these the most frequent rearrangements are *TPM3/NTRK1* [83], *TPR/NTRK1* [82, 84] and *TFG/NTRK1* [85]. *NTRK1* rearrangements are reported in ~5% of PTCs [77], with a NTRK1 molecular activations similar as those described for RET [86].

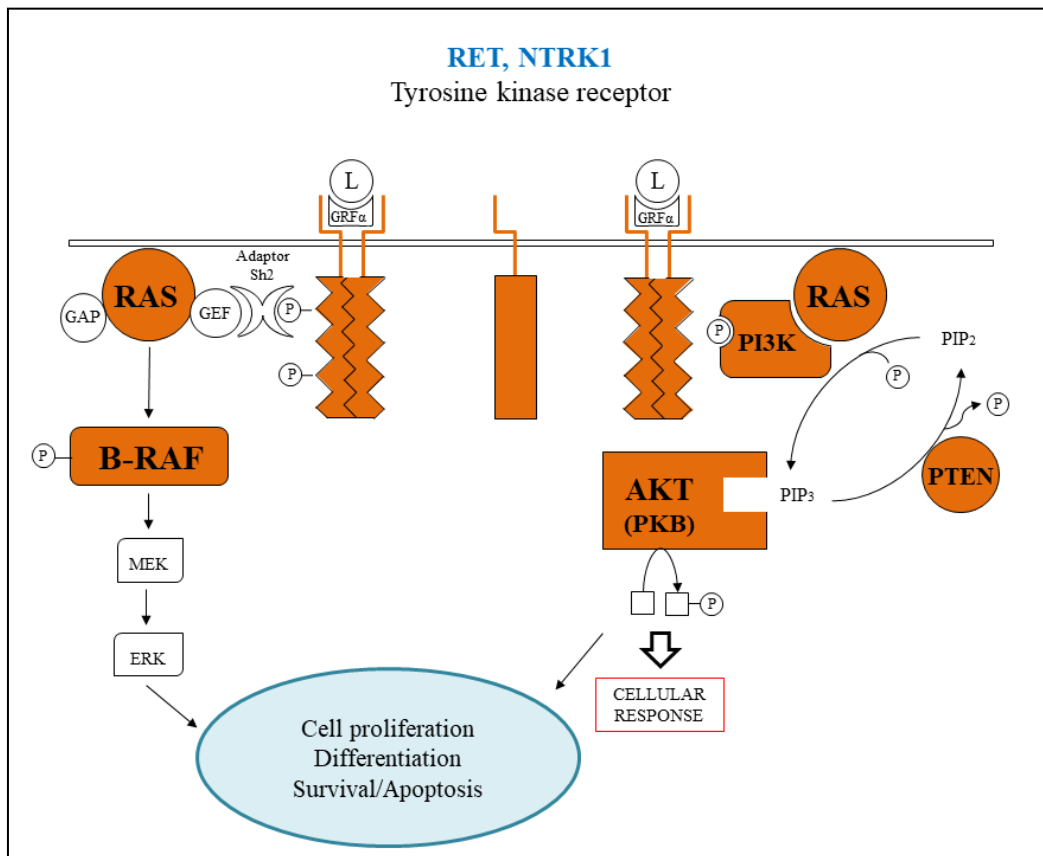


Figure 5: Many of the molecules altered in thyroid cancers (in orange) involving MAPK cascade (left and PI3K/PTEN/AKT pathway (right).

RAS: small GTPase RAS protein; GAP: GTPase activating protein; GEF: guanine nucleotide exchange factor; adaptor SH2: adaptor proteins with Src homology regions; B-RAF: protein kinase BRAF (mitogen-activated protein 3 kinase, MAP3K); MEK: mitogen-activated protein Erk kinase (mitogen-activated protein 2 kinase, MAP2K); ERK: extracellular-signal-regulated kinase (mitogen-activated protein kinase, MAPK); L: ligand; GFRα: GDNF-family α coreceptor; PI3K: phosphoinositide 3-kinase; AKT: AKT kinase (also known as PKB).

The *NTRK3* is located on long arm of the chromosome 15 (15q25.3), and encodes NTRK3 which binds the neurotrophin-3 (NT3) growth factor with high affinity. Similarly to NTRK1, NTRK3 is not physiologically expressed in the thyroid cells, while it is expressed in the CNS.

The most frequent rearrangement is *NTRK3* fusion to the *ETS variant gene 6* (*ETV6*), resulting in the *ETV6/NTRK3* oncogene. *ETV6/NTRK3* seems to be the most frequent chromosomal rearrangement after *RET/PTC* in radiation-associated thyroid neoplasms, reported in ~15% of radiation-induced PTCs, typically in cases with follicular architecture (classic PTC with a component of follicular growth or follicular variant PTC)[87, 88]. *ETV6/NTRK3* rearrangement has been reported in approximately 2% of PTCs not associated with radiation. *ETV6/NTRK3* was observed in many different neoplasia, as congenital fibrosarcoma, congenital mesoblastic nephroma, and secretory carcinomas of the breast and salivary gland; however, in PTC it shows the fusion points of the chimeric products (usually *ETV6* exon 4-*NTRK3* exon 14) different from those observed in most extrathyroid neoplasms (*ETV6* exon 5-*NTRK3* exon 13) [87] .

Two other *NTRK3* rearrangement were also reported: *RBPM5/NTRK3* [63] and *SQSTM1/NTRK3* [18].

NTRK-rearrangement is a typical alteration found in PTCs from young patients and children, with lymph node metastases and aggressive behavior, similarly to *RET*-rearranged cancers [78, 79].

3.2.1.3 *ALK* (anaplastic lymphoma kinase)

ALK is located in the short arm of chromosome 2 (2p23) and encodes a transmembrane tyrosine kinase receptor. Through the binding with its ligands pleiotrophin (PTN) and midkine (MK), both growth factor, *ALK* plays an active role in the development of the central and peripheral nervous systems [89]. The first evidence of *ALK* as an oncogene was in 1994, when it was found to be fused to *NPM1* in an anaplastic large-cell non-Hodgkin's

lymphomas (ALCL) [90]. Since then, different tumors harboring *ALK* alterations (including rearrangement, mutation, and amplification) were identified, such as non-small cell lung carcinoma (NSCLC), mesenchymal neoplasms, and neuroblastoma [91]. When it is altered, *ALK* is aberrantly activated and promotes cell proliferation and survival through MAP kinase and PI3K/PTEN/AKT pathways (**Figure 5**) [92, 93].

ALK rearrangements seem to be in association with radiation exposure and aggressive clinical-pathological features. *ALK* is fused to *EML4* in ~13% of PTC with solid/trabecular architecture, high radiation dose, and younger age [94]. *ALK/STRN* was described in 9% percent of PDTC and in 4% of ATC [95, 96]. A small percentage of PTCs (~1%) harbors *STRN/ALK*, and these tumors show a predominance of follicular growth pattern [95]. With a lower frequency, other 5 *ALK* rearrangement were describe in high grade thyroid cancers [64, 68, 97, 98].

ALK rearrangements could be a predictive marker because patients with *ALK*-rearranged cancers may respond to target therapies with *ALK* inhibitors (e.g. crizotinib) [95].

3.2.2 BRAF

The RAF family includes three different isoforms of serine-threonine kinase: ARAF, BRAF, and CRAF (also called RAF-1) [99]; they are all intracellular effectors of the MAPK signal transduction pathway (**Figure 5**). Structurally, the RAF proteins present three conserved regions (CR): CR1 and CR2 at the N-terminus and CR3 at the C-terminus [100, 101]. The RAS-binding domain (RBD) is in CR1, while CR2 is a serine/threonine rich domain, containing a site, when phosphorylated, that can bind to 14-3-3, a regulatory protein. CR3 contains the kinase domain responsible for RAF activation and MEK1/2 phosphorylation. In CR3 domain there is the important aspartate-phenylalanine-glycine (DFG) motif, which plays a fundamental role for the regulation of the ATP-binding pocket [100]. Activating mutations, such as *BRAF* p.V600E, can destabilize and disrupt

the inactive conformation of the DFG motif, resulting in a constitutively activated protein state [102].

The *BRAF* gene (v-raf murine sarcoma viral oncogene homolog B) is located on the long arm of chromosome 7 (7q34) and encodes a full-length protein of 766 amino acids (94 kDa) [99, 103, 104]. Since the discovery of activating alterations, *BRAF* was found to be mutated in malignant melanoma (27%-70%), thyroid cancers (40-45%), colorectal cancer (5%-22%), serous ovarian cancer (~30%) and in other human cancers with a lower frequency (1%-3%) [105-108]. Activating point mutations of *BRAF* occur in the kinase domain encoded by exons 11 and 15. Differently from other cancers, no mutations in exon 11 were found in thyroid neoplasia [105-107, 109]. Mutated *BRAF* proteins have been divided into three groups, according to the activation of downstream molecules, such as MEK: i) high activity (i.e. p.V600E and p.K601E); ii) intermediate activity; iii) impaired activity [102]. Unlike the *BRAF* p.V600E substitution, the mechanism of activation of downstream protein in MAPK pathway through which “uncommon” *BRAF* mutants act is not fully understood.

Among the alterations observed in *BRAF*, ~95% consists in a point mutation in exon 15, that involves nucleotide 1799 (thymine to adenine transversion, c.1799T>A), resulting in a valine to glutamate substitution at residue 600 (p.V600E) [20, 110, 111]. *BRAF* p.V600E mimics the phosphorylation of the activation segment, that results in a constitutive activation of *BRAF*.

BRAF p.V600E is typically found in PTC with a tall cell architecture (80%) or with a classical histology (60%), while it is rarely observed in the follicular variant of PTC (10%) [20, 110, 112, 113], in which point mutation other than *BRAF* p.V600E (e.g. p.K601E) are found [114, 115]. Therefore, the presence of these mutations can be used as a diagnostic marker for PTC. *BRAF* p.V600E has also been described in PDTC and ATC (24%), especially in those derived from *BRAF* p.V600E positive tumors [116].

Several studies have shown a correlation between this alteration and a worst outcome for *BRAF* p.V600E -positive patients, and it was demonstrated to be a poor prognostic factor independent from other clinic-pathological

features [117-119]. Whereas, other studies have not confirmed the role of *BRAF* p.V600E as a tumor aggressiveness-related factor [120-122]. For these reasons, the prognostic role of *BRAF* p.V600E is still controversial.

BRAF p.V600E is also considered a predictive marker: tumor harboring this alteration respond to kinase inhibitor (dabrafenib and vemurafenib) [123].

Other non- *BRAF* p.V600E mutations are reported in 1-2% of PTC; they include other point mutations, small ins/del and chromosomal rearrangements [124]. Among point mutations, *BRAF* p.K601E is related to neoplasm with a follicular architecture: it was detected in FA and in 7-10% of the follicular variant of PTC [49, 125]. Twenty-one different *BRAF* rearrangements have been reported in relation with PTC or high grade thyroid cancers [63, 68, 126-129].

3.2.3 RAS

The *H-RAS*, *N-RAS* and *K-RAS* oncogenes belong *RAS* superfamily, composed by more than 150 21-kDa G proteins that play a crucial role in MAPK and PI3K/PTEN/AKT pathways (**Figure 5**), contributing to the control of proliferation, differentiation, and survival of eukaryotic cells [130]. As a G-protein, RAS proteins cycle between active GTP-binding form and inactive GDP-binding states, with a highly conserved mechanism. The conversion from the inactive form to the active one is under the stimulation of GEFs, while the conversion to the inactive form is controlled by GAPs.

Besides cancers, alteration in RAS signaling are known to be involved in the development of many pathologies, such as non-obese diabetes and diabetic retinopathy, hyperinsulinemia [131-133], glomerulonephritis [134].

Activating *RAS* point mutations are concentrated in two hotspot of the primary nucleotide sequence of all *RAS* family members. They can affect the GTP-binding domain (exon 2, codons p.G12 or p.G13) or the GTPase domain (exon 3, codon p.Q61) which “lock” the protein in the active GTP-bound form and constitutively activate the protein [135, 136]. Constitutive activation of *KRAS*, *NRAS*, and *HRAS* is one of the most common events in

human tumorigenesis. About 30% of all human neoplasia is found to harbor mutation in any of the canonical *RAS* genes, predominantly *K-RAS* (25-30%), while *N-RAS* and *H-RAS* occur with lower frequency (8% and 3%, respectively) [137]. In thyroid tumor, mutation in *RAS* oncogenes are described in those whose arised from the follicular epithelium, predominantly with a follicular growth pattern. It has been reported in 5-10% of hyperplastic thyroid nodules [138] and in 20-50% of follicular carcinoma, follicular adenoma, and the follicular variant of papillary carcinoma [20]; while they are uncommon in conventional papillary carcinomas. The high frequency in both PDTC and ATC could indicate their involvement in progression and their association with carcinomas with aggressive clinic *BRAF* p.V600E -pathologic features and poor prognosis [139-141].

Oncogenic *RAS* activation also occurs in medullary carcinoma, and it seems to be mutual exclusive with that of *RET* [142-144]. The more frequently mutations are in *H-RAS* and *K-RAS* genes, while *N-RAS* mutations are quite uncommon [136, 142-144].

3.3 PI3K/PTEN/AKT PATHWAY

The PI3K/AKT/PTEN pathway has an important role in regulating metabolism, cell growth, and cell survival as well as carcinogenesis, tumor growth and angiogenesis [145]. When the ligand bind its TRK, the receptor starts the dimerization, and subsequently increases PI3K activity in producing both phosphatidylinositol-3,4-diphosphate (PIP2) and phosphatidylinositol-3,4,5-triphosphate (PIP3). These events active PDK1 and AKT which is involved in the regulation of multiple cellular functions (metabolism, protein synthesis, cell cycle progression, anti-apoptosis, tumor growth, and angiogenesis) through different downstream targets (**Figure 5**).

The **PI3K** family comprehend signal transducer enzymes responsible of PIP2 and PIP3 production and AKT activation. They are divided into three classes (class I, class II, and class III); the production of PIP3 is a unique

activity of class I, which consists in proteins activated by RTKs (class IA) or G-protein-coupled receptors (class IB) [146]. PI3K presents a catalytic subunit (p110), which generates PIP3, and a regulatory subunit (p85), involved in receptor binding and activation / localization of the enzyme. In class IA three genes, *PIK3CA*, *PIK3CB* and *PIK3CD*, are involved in encoding p110 isoforms: p110 α , p110 β and p110 δ , respectively. Subunit p110 α and p110 β are known to be ubiquitously expressed, while p110 δ is expressed only in immune system [147-149].

AKT (protein kinase B [PKB]) is a family of serine/threonine-specific protein kinases which is the major downstream target of PI3K. In human, AKT presents three isoforms, AKT1, AKT2, and AKT3 [150]; all of them are expressed in the normal thyroid, but AKT1 and AKT2 are the most abundant [151, 152]. Once PIP3 binds and activates phosphoinositide-dependent kinase 1 (PDK1), PDK1 phosphorylates AKT in the kinase domain, represented by the residue Thr308 in AKT1. AKT1 is fully activated by the additional phosphorylation Ser473, involving PDK2 [153]. The active form of AKT phosphorylates several downstream targets such as mTOR complex [154], playing an important role in regulation of various cellular functions, including proliferation, survival, and metabolism.

PTEN (phosphatase and tensin homolog deleted on chromosome 10) is a dual function protein: it acts as phosphatase on protein and lipid, and negatively regulates the activity of PI3K/AKT signaling through the dephosphorylation of phosphoinositide substrates and the conversion of PIP3 to PIP2 [155]. For this reason *PTEN* (localized in 10q23.31) is a tumor suppressor, which it is often inactivated through different mechanisms.

Deregulation of PI3K/PTEN/AKT pathway is known to be associated with tumor progression in thyroid cancer: this is a common alteration found in high grade cancers, with an aggressive behaviour (PDTC and ATC). Activating somatic point mutations of PI3K are described in *PIK3CA* (mapped in 3q26.3), clustered in exon 9 (encoding for the helical domain) and in exon 20 (encoding for the for kinase domain). *PIK3CA* copy number gains are also known, but their tumorigenic role is less defined. Point

mutations have been reported in 0-10% of FTC and in 0-25% of PDTC and ATC, while copy number gains were identified in approximately 25% of FTC and in 40% of ATC, but their tumorigenic role is less defined [156-159].

Alteration in AKT signaling are caused both by dysregulation of PI3K function, as well as *PTEN* Loss of Function (LOF) alteration [157]. Moreover, mutations in *AKT1* are known to constitutively activate AKT signaling 15% of high-grade, aggressive, radioactive iodine-refractory forms of thyroid cancer [160].

PTEN mutations have been reported in sporadic thyroid tumors in 0-10% of FTC and in 5-20% PDTC and ATC. However, loss of heterozygosity or epigenetic mechanisms (such as *PTEN* promoter methylation) are a more common in cancer, causing the decreased of *PTEN* mRNA and protein levels [157, 161-164]. Germline *PTEN* LOF mutations are responsible for Cowden syndrome, an autosomal dominant condition characterized by multiple benign tumors and hamartomatous proliferations at various sites [165].

3.4 PPAR γ REARRANGEMENT

PPAR γ (peroxisome proliferator-activated receptor γ) belongs to the nuclear receptor family of transcription factors, involved in regulation of lipid metabolism (adipogenesis) and insulin sensitivity [166, 167]. *PPARG* maps in the short arm of chromosome 3 (3p25.2) and encodes for protein with a classical nuclear hormone receptor structure: a N-terminal regulatory “AB” domain; centrally it shows a zinc finger DNA binding domain, and a ligand binding/transcriptional regulatory domain at the C-terminal (**Figure 6.A**). Two isoforms, PPAR γ 1 and PPAR γ 2, are known, and they seem to have a similar function, but they differ for 30 amino acid (PPAR γ 2 is longer than PPAR γ 1) and they have a different expression pattern (PPAR γ 2 is expressed specifically in adipocytes). In thyroid, PPAR γ expression level

tends to be very low, but it becomes higher when *PAX8/PPAR γ* rearrangement is detected [168, 169].

PAX8 (paired box gene 8) belongs to a transcription factor family, involved in the genesis and differentiation of thyroid follicular cell, driving the expression of many thyroid-specific genes such as those encoding thyroglobulin, thyroid peroxidase and the sodium iodide symporter [170]. *PAX8* gene consists in 12 exons, with the DNA binding domain (DBD) encoded by exons 3, 4 and the beginning of exon 5, while the transcriptional activation domain is encoded by exons 10 and 11 (**Figure 6.B**). Alternative splicing of exons 8-10 results in 5 protein isoforms, PAX8A, B, C, D and E, among which PAX8A is the longest isoform and includes all codons from exons 2-12. PAX8B is shorter than PAX8A because of the deletion of exon 9, without the alteration of the reading frame of downstream exons. PAX8C presents a smaller exon 9, derived from an alternative splicing; the result of this event is a altered reading frame shift, with the stop codon in exon 11. Both PAX8D and PAX8E are shorter than PAX8C (PAX8D harbors the deletion of exons 8 and 9, while PAX8E is deleted in exons 8, 9 and 10), but they show the same reading frame shift of PAX8C [171].

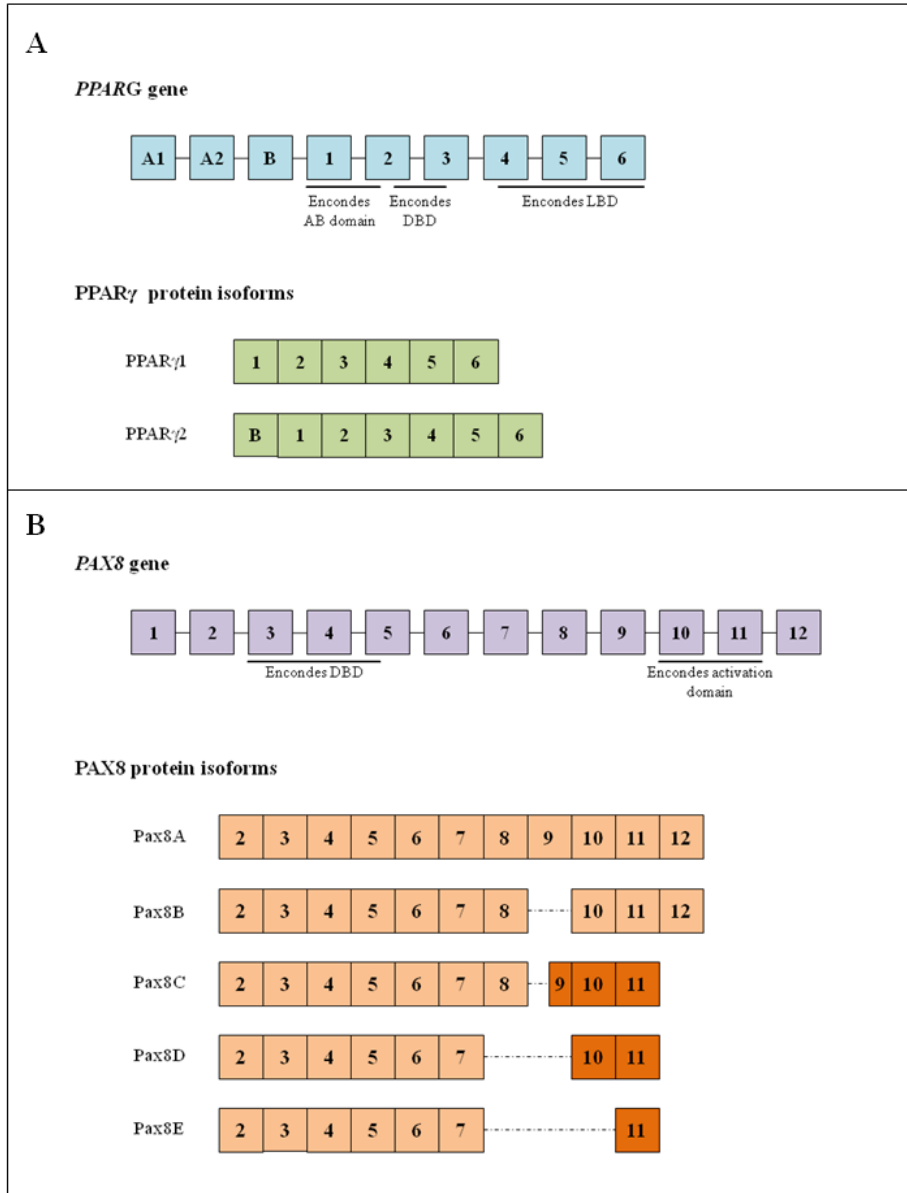


Figure 6: Schematic representation of the PPARG gene (A) and PAX8 gene (B). The exons are not drawn to scale. A) Coding exons are shown in blue, noncoding in white, while the protein is in green. Only the PPARG exons that contribute to the PPAR γ 1 protein are shown, and for convenience they are numbered starting at 1 (the gene has several additional upstream exons). B) Coding exons are shown in violet, noncoding in white, while the protein is in orange. The reading frame shift is shown by a darker shade of orange within the exons. DBD: DNA binding domain; LBD: ligand binding domain/transcriptional regulatory domain.

The *PAX8/PPARG* rearrangement is a translocation involving the long arm of chromosome 2 and the short arm of the chromosome 3 [t(2;3)(q13;p25)] (**Figure 7**) [172]. This alteration results in a fusion transcript wherein most of the coding sequence of PAX8 (including its promoter region) is fused in frame with the entire coding exons of PPAR γ 1. Because of the high activity of PAX8 promoter, PAX8/PPAR γ Fusion Protein (PPFP) is highly expressed in follicular thyroid cells harboring this translocation [173].

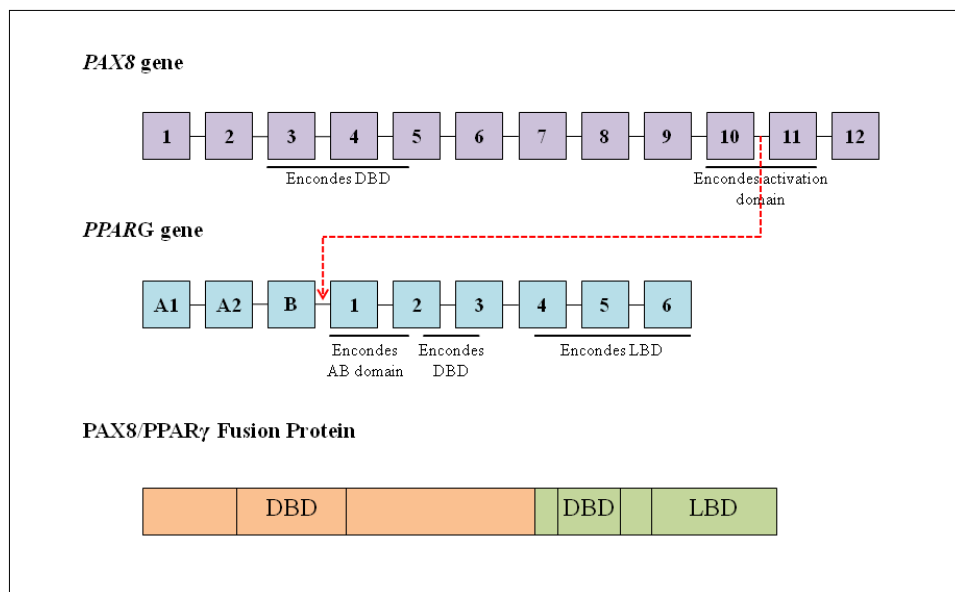


Figure 7: Schematic representation of PAX8/PPAR γ Fusion Protein (PPFP). Typically, the fusion involve PAX8 exons 1-10 with the entire sequence of PPAR γ 1. The resulting PPFP consists of an N-terminal PAX8 fragment encoded by exons 2-10 fused in frame to full length PPAR γ 1. The PAX8 portion is essentially a truncated version of PAX8A, missing much of the C-terminal activation domain. Not shown, PAX8 variants result in alternative isoforms of PPFP that only include PAX8 exons 1-8, or 1-9, or 1-10 without exon 9. DBD: DNA binding domain; LBD: ligand binding domain/transcriptional regulatory domain

A second rearrangement of the *PPARG* involves the gene *CREB3L2* (mapped at 7q34) [t(3;7)(p25;q34)]: the fusion results in *PPARG* fused in frame with *CREB3L2* exons 1 and 2 [174]. *CREB3L2/PPARG* is much less common than *PAX8/PPARG*, with an estimated prevalence lower than 3 percent among follicular carcinomas. It has been reported in one radiation-associated follicular variant papillary carcinoma that developed in a child

exposed to the Chernobyl radioactive fallout [88]. *CREB3L2/PPARg* has not been identified in benign or non-malignant thyroid tissue [88].

PAX8/PPARG typically occurs in follicular-patterned neoplasias: it is reported in 20-50% of FTC, in FTA and in PTC-EFV, but with a lower and variable frequency [175-178]. *PAX8/PPARG* is very rare in PDTC and ATC [97, 160].

CREB3L2/PPARG has been reported with a lower frequency (~3%) in FTC and in ~1.5% of PTC-EFV [179].

Aim of the study

This study has two Aims.

Aim1. The molecular profile of Papillary Thyroid Carcinomas has been deeply investigated. However, to date, there are no informations regarding the molecular profile of the non-malignant tissue surrounding the PTC. Exploring the molecular signature, and in particular the *BRAF* status, of the non- neoplastic tissue surrounding the tumor may help to better understand thyroid tumorigenesis and the events that lead potential precursor lesions to evolve to papillary carcinoma.

The first aim of this project is to establish whether *BRAF* mutations are present in non-malignant tissue surrounding PTC, and in case they are found to characterize their activity in vitro.

Aim 2. The combination of cytologic analysis and molecular testing is improving the pre-operative evaluation of thyroid nodules. The definition of molecular panels can be very useful to inform treatment, to establish the best surgical approach, and to stratify patient risk.

The second aim of this project is to set up a RNA based expression panel that may provide diagnostic, predictive and prognostic information on thyroid nodules/neoplasms.

Next Generation Sequencing techniques, mutagenesis, cell transfection, and protein functional assays were used to achieve these aims.

Materials and Methods

Aim 1: Detection of BRAF mutations in neoplastic and non-malignant tissue and analysis of BRAF-mutant activity

1 NEXT GENERATION SEQUENCING

1.1 CASES SELECTION

In the present study, we analyzed the *BRAF* molecular status of 30 PTCs including 100 areas from tissues surrounding the tumor. The age of the patients ranged from 29 to 79 years (mean 48.3 years; median 49.0 years). Ten patients were male (33.3%) and 20 were female (66.7%) (**Table 1**).

Non-malignant tissues were classified as following (**Table 1**): i) characterized by the presence of hyperplasia (“HYP”- n=16); ii) characterized by the presence of “atypia” (“ATY” - n=38). Atypical thyroid tissue was defined by the presence of unusual features, including follicular cells showing some crowding and minor alterations of the nuclear morphology, such as mild nuclear clearing, mild enlargement and contour irregularities, similar to what described in multifocal fibrosing (sclerosing) thyroiditis [180]; iii) areas containing psammoma body (“PsB” - n=6); iv) tissue with typical thyroidal architecture (“NORM” - n=34);

Malignant neoplasia analyzed in this study were: i) 15 PTC-CL (50.0%); ii) 9 PTC-FV (30.0%); iii) 5 PTC-TC (16.7%); iv) one sclerosing PTC (3.3%) (**Table 1**). Moreover, the following areas with non-malignant neoplasia were analyzed: i) follicular adenoma (“FA” - n=4); ii) follicular adenoma with oncocytic features (“FA-OC” - n=2) (**Table 1**).

Features	n	% (n=30)
<i>Sex</i>		
Male	10	33.3
Female	20	66.7
<i>Malignant histotype</i>		% (n=30)
PTC-CL	15	50.0
PTC-FV	9	30.0
PTC-TC	5	16.7
Sclerosing PTC	1	3.3
<i>Non-malignant tissue</i>		% (n=100)
ATY	38	38,0
HYP	16	16,0
NORM	34	34,0
FA	4	4,0
PsB	6	6,0
FA-OC	2	2,0

Table 1: Features of cases.

1.2 DETECTION OF *BRAF* MUTATIONS

1.2.1 DNA extraction and quantification

All samples were formalin-fixed and paraffin-embedded (FFPE) and were retrieved from the archives of Anatomic Pathology Unit of Bellaria and Maggiore Hospital (Bologna, Italy) from 2009 to 2011.

DNA was extracted from two to four 10- μ m-thick sections using the HighPure PCR Template Preparation Kit (Roche-Diagnostic, Mannheim, Germany), scraping the area of interest with a sterile blade, according to the selection performed by the anatomic pathologist on the haematoxylin and eosin (H&E) stained slide.

The concentration of the extracted DNA was assessed using the Quant-iT™ dsDNA BR Assay Kit using a Qubit™ Quantitation Platform (ThermoFisher Scientific, Waltham, MA, USA).

1.2.2 Amplicon library preparation

Next Generation Sequencing (NGS) was performed using the 454 GS-Junior (Roche Diagnostic), according to the manufacturer's instruction (<http://www.454.com/>).

Briefly, at least 10 ng of DNA was amplified targeting *BRAF* exon 15, using the following primers: Sense 5'-TGCTTGCTCTGATAGGAAAATGA-3' and Antisense 5'-TGGATCCAGACAACCTGTTCAA -3' (Table 5).



Figure 8: 454 Next-Generation Sequencing primers.

Primers were modified and they were made up to 3 parts (Figure 8):

- a universal sequencing tail (A and B) is composed of an adaptor and a “key”. The adaptor sequences (A and B) are involved the EmPCR. The “key” is composed of a four nucleotide sequence (TCAG) that allows the instrument to recognize where the amplicon sequence starts;
- multiple identifiers nucleotide sequences (MIDs) are a unique DNA barcode that allows the instrument to identified each sample;
- template specific sequence.

PCR conditions (both reaction mix and amplification steps) are reported in Table 2.

<i>Reaction mix (final volume 25μl)</i>		
<i>Reagent</i>	<i>Concentration</i>	
dNTP (Roche)	0.2 mM	
FastStart High Fidelity Reaction Buffer	1X	
MgCl ₂ Solution	1mM	
FastStart High Fidelity Enzyme Blend	1.25 U	
Primers (both FW and REV)	6.25pmol	
Molecular biology grade water	-	

<i>PCR steps</i>		
<i>Temperature (°C)</i>	<i>Time</i>	<i>No. of cycles</i>
95	2'	1
95	30"	37
60	30"	37
72	1'	37
72	7'	1

Table 2. Reaction mix and PCR steps used for amplicon library preparation.

1.2.3 Library purification and quantification

For the amplicon library purification magnetic beads were used (Agencourt AMPure XP PCR Purification, Beckman Coulter). Briefly, PCR products were mixed and incubated at room temperature with magnetic beads. Then, in order to separate amplicons bound to magnetic beads from contaminants, a magnet was used (Agencourt SPRIplate 96 Super Magnet Plate).

After two washes with ethanol 70%, amplicons were eluted in 20 μ l of 1x TE Buffer (10 mM Tris-HCl pH 8.0, 1 mM EDTA, Sigma-Aldrich).

Purified amplicons were then quantified using the Quant-iT PicoGreen® dsDNA quantitation Assay Kit (ThermoFisher Scientific, Waltham, MA, USA) and measured with the QuantiFluor®-ST Fluorometer (ThermoFisher Scientific).

1.2.4 Amplicons dilution, pooling and EmulsionPCR

Based on the concentration, amplicons were diluted with 1x TE Buffer in order to obtain 1×10^9 molecules/ μl per each well. The amplicon were pooled and further diluted in molecular biology grade water to reach the desired concentration.

An EmulsionPCR (EmPCR) were carried out. Briefly, two identical reaction mix (**Table 3**), except for sequencing primers, were prepared. After 2 washes, amplicons dilution (12 μl) and both mix A and B (600 μl) were added to *Capture Beads A* and *Capture Beads B*, respectively.

<i>Reaction mix (final volume 600 μl)</i>		
<i>Reagent</i>	<i>Volume (μl)</i>	
Additive	260	
Molecular biology grade water	205	
Enzyme Mix,	35	
Amp Mix	135	
PPiase	1	
Primers (A and B)	40	

<i>PCR steps</i>		
<i>Temperature ($^{\circ}\text{C}$)</i>	<i>Time</i>	<i>No. of cycles</i>
94	4'	1
94	30"	50
56	4'30"	50
68	30"	50
10	Up to 16h	1

Table 3: *Reaction mix and steps used for EmPCR.*

1.2.5 Recovery and enrichment

The emulsion was broken and beads recovered. In order to separate DNA-carried beads from mixed or empty one, an enrichment process was performed. Briefly, after an incubation with a Melt Solution (containing NaOH), "*Capture Beads*" were then incubated with biotinylated *Enrich Primer A* and *Enrich Primer B*. Using streptavidin-coated magnetic beads

(*Enrichment Beads*) and a *Magnetic Particle Concentrator (MPC)*, “empty” (i.e. without amplicons) beads were separated and discarded.

Sequencing Primers were added to the beads, and aliquoted to a *PicoTiterPlate (PTP)* with *Packing Beads*, *Enzyme Beads* and *PPIase beads*. The sequencing was then carried out.

Results were analyzed using Amplicon Variant Analyzer (AVA) software (Roche Diagnostic, Mannheim, Germany). Only nucleotide variations observed in both strands, with at least 1% of allele-read were considered for the mutational calling

2 SITE-DIRECT MUTAGENESIS AND CELL TRANSFECTION

2.1 MUTANT BRAF PLASMIDS GENERATION VIA SITE-DIRECTED MUTAGENESIS

The construct pCMV6 encoding wild-type BRAF (#40775) was purchased from Addgene (Cambridge, MA USA) in frame with the tag FLAG. Mutations p.G593D, p.A598T, p.V600E, p.K601E, p.S607F and p.S607P were inserted using the Q5 Site-direct Mutagenesis kit, according to the manufacturer’s instruction (New England Biolabs, Ipswich, MA, USA). The oligonucleotides used for the mutagenesis are reported in **Table 5**. Briefly, 1-25 µl of template were amplified using conditions reported in **Table 4**.

<i>Reaction mix (final volume 25 μl)</i>		
<i>Reagent</i>	<i>Concentration</i>	
Q5 Hot Start High-Fidelity 2X Master Mix	1X	
Primer FW (10 μ M)	0.5 μ M	
Primer RV (10 μ M)	0.5 μ M	
Template DNA	1–25 ng/ μ l	
Molecular biology grade water	-	

<i>PCR steps</i>		
<i>Temperature ($^{\circ}$C)</i>	<i>Time</i>	<i>No. of cycles</i>
98	30''	1
98	10''	25
60	30''	25
72	30''	25
72	2'	1
10	-	1

Table 4: *Reaction mix and steps used for mutagenesis.*

Amplified plasmidic DNA were incubate with Kinase-Ligase-DpnI (KLD) enzymes and competent cell (NEB 5-alpha Competent E. coli) were transformed.

Plasmid DNA extraction were performed using Plasmid *Plus* Midi Kit (QIAGEN, Germantown, MD, USA) following manufacturer's instructions.

The site-directed mutagenesis was verified by plasmid direct sequencing (PE Applied Biosystems) using *BRAF* exon 15-targeting primers (all reported in **Table 5**).

BRAF (Ex15) NGS 454 GS-Junior primers

BRAF FW: TGCTTGCTCTGATAGGAAAATGA

(Ex15) RV: TGGATCCAGACAACTGTTCAAA

Mutagenesis primers

p.G593D FW: GTAAAAATAGATGATTTTGGTCTAGC

RV: TGTGAGGTCTTCATGAAG

p.A598T FW: TTTTGGTCTAACTACAGTGAAATC

RV: TCACCTATTTTTACTGTGAG

p.V600E FW: CTAGCTACAGAGAAATCTCGATG

RV: ACCAAAATCACCTATTTTTAC

p.K601E FW: AGCTACAGTGGAAATCTCGATG

RV: AGACCAAATCACCTATTTTTAC

p.S607F FW: TGGAGTGGGTTCCATCAGTT

RV: TCGAGATTTCACTGTAGCTAG

p.S607P FW: ATGGAGTGGGCCCATCAGTT

RV: CGAGATTTCACTGTAGCTAG

BRAF (Ex15) Sanger sequencing primers

BRAF FW: ACACGCCAAGTCAATCATCC

(Ex15) RV: TCTGACTGAAAGCTGTATGGATT

Table 5:Primer used for NGS 454-gs Junio, mutagenesis, Sanger sequencing and vector sequencing. In bold the nucleotide involved in the mutation

2.2 CELL TRANSFECTION

For transient transfection, 4×10^5 cells HEK293 were seeded in complete medium and incubated at 37 °C in a humidified atmosphere with 5% CO₂. After 24 hours, 4 µg of *BRAF* mutant plasmids were transfected using liposomes according to the manufacturer's instructions (Lipofectamine 3000, ThermoFisher Scientific). 48 hours after transfection, cells lysates were produced using RIPA buffer.

3 WESTERN BLOT

Cells were lysed in ice-cold RIPA buffer: 50 mM HEPES (EuroClone, Milan, Italy), 1 mM EDTA (Sigma-Aldrich), 10% glycerol (ThermoFisher

Scientific), 1% Triton X-100 (Sigma-Aldrich), 150 mM NaCl in the presence of proteases and phosphatases inhibitors (Sigma-Aldrich).

Total protein was measured using the Lowry protein assay kit (Biorad DC Protein Assay; Biorad, Hercules, CA USA) according to the manufacturer's instruction. Protein samples (15 µg) were subsequently separated 4-20% pre-cast gels (ThermoFisher Scientific). Gels were then electro-transferred onto nitrocellulose membranes (Trans-Blot Turbo Transfer System, Biorad). Membranes were blocked in Tris Buffered Saline (TBS) with 1% Casein (Biorad) for 1 hour at room temperature and incubated with primary antibodies at 4°C overnight. Membranes were washed three times in Tris-buffered saline containing 0.1% Tween and incubated with peroxidase-conjugated secondary antibodies for 45 minutes at room temperature.

Bands were visualized using WESTAR Supernova (Cyanagen, Bologna, Italy) and detected with the ChemiDoc™ XRS+ (Biorad). Densitometric analysis have been performed with ImageLab software (Biorad).

Primary antibodies were used against: phospho-ERK (Thr202/Tyr204) (rabbit, 1:1000), total ERK (mouse, 1:1000), phospho-MEK (Ser217/221) (rabbit, 1:250), total MEK (mouse, 1:250), phospho-BRAF (Ser445) (rabbit, 1:250), total BRAF (rabbit, 1:250), vinculin (mouse, 1:10,000), γ -tubulin (mouse, 1:10,000) (all purchased by Cell Signalling, Leiden, Netherlands) and FLAG tag (mouse, 1:10,000, Sigma-Aldrich). Peroxidase-conjugated secondary antibodies used were: anti-mouse IgG (1:10,000; Sigma-Aldrich) and anti-rabbit IgG (1:10,000; Sigma-Aldrich) (**Table 6**).

<i>Primary Antibody</i>				
Antibody	Weight (KDa)	Dilution	Animal origin	Source
anti-phospho-ERK (Thr202/Tyr204)	42-44	1:1000	Rabbit	Cell Signaling Technology
anti-ERK	42-44	1:1000	Mouse	Cell Signaling Technology
anti-phospho-MEK (Ser217/221)	45	1:250	Rabbit	Cell Signaling Technology
anti-MEK	45	1:250	Mouse	Cell Signaling Technology
anti-phospho-BRAF (Ser445)	94	1:250	Rabbit	Cell Signaling Technology
anti-BRAF	94	1:250	Rabbit	Cell Signaling Technology
anti-FLAG	94	1:1000	Mouse	Sigma-Aldrich
anti- γ -Tubulina	46	1:10000	Mouse	Cell Signaling Technology
Vinculin	102	1:10000	Mouse	Cell Signaling Technology
<i>Secondary Antibody</i>				
anti-mouse IgG	-	1:10000	-	Sigma-Aldrich
anti-rabbit IgG	-	1:10000	-	Sigma-Aldrich

Table 6: Primary and secondary antibody use in Western Blot analysis.

Aim 2: Design and set up of a gene expression panel.

4 GENE PANEL DESIGN

The RNA-based expression panel was designed to detect fusion and to identify dysregulated expression of genes known to be altered in thyroid cancer, and with the potential for diagnostic and clinical relevance.

For this RNA-based panel, primers were designed to detect 30 gene fusions, 9 expressed fusion genes, 16 genes involved in biomarker and thyroid lineage and differentiation, 18 genes involved in immune-oncology, 42 genes differently expressed in BRAF-like or RAS-like cancers, 5 genes up/down regulated in cancers, 38 proliferation genes. Moreover, 27 housekeeping genes were included (**Table 7** and **Supplementary Table 1**).

Main pathways related to genes investigated	No.	Breakpoints
Gene Fusion	30	93
Expressed fusion	9	-
BRAF-like signature	22	-
RAS-like signature	16	-
RET signature	4	-
Down/Up regulated in carcinoma	5	-
Immuno-oncology	18	-
Lineage	6	-
Biomarker	2	-
Thyroid differentiation score	8	-
Proliferation	38	-
Housekeeping	27	-

Table 7. Genes included in the panel.

5 SELECTION OF CASES

We analyzed 44 fresh-frozen (FF) samples to test our expression panel.

Forty-one FF specimens were from thyroid gland. The age of the patients ranged from 15 to 82 years (mean 43.5 years; median 43.0 years). Ten of 41 patients were male (24.4%) and 31 were female (75.6%).

FF specimens included (**Table 8**): i) normal thyroid tissue (n=3); ii) hyperplastic thyroid tissue (n=4); iii) follicular adenoma (n=3); iv) Hürthle cell carcinoma (n=3); v) PTC-CL (n=9); vi) PTC-TC (n=5); vii) PTC-FV (n=5); viii) FTC (n=4); ix) ATC (n=3); x) MTC (n=1).

Four sample of colo-rectal cancer (CRC) were analyzed as control.

Thyroid Tissue (n=41)	BRAF positive	RAS positive	PAX8/PPARG positive	WT
Normal tissue (n=3)	-	-	-	3
Hyperplastic tissue (n=4)	-	-	-	4
Follicular adenoma (n=3)	-	2	-	1
Hürthle cell carcinoma (n=3)	-	-	-	3
PTC-CL (n=9)	9	-	-	-
PTC-TC (n=5)	5	-	-	-
PTC-FV (n=5)	1	4	-	-
FTC (n=4)	-	-	3	1
ATC (n=3)	2	-	-	1
MTC (n=1)	-	-	-	1

Table 8. *Fresh Frozen specimens tested for the custom RNA-based panel.*

6 NEXT GENERATION SEQUENCING

6.1 DNA AND RNA EXTRACTION

Fourty-four FF samples were analyzed. They were all retrieved from the archives of Pathology Unit of the University of Michigan (Ann Arbor, Michigan, USA) from 1995 to 2003. All samples were previously characterized using Affymetrix microarray analysis (ThermoFisher).

DNA and RNA were extracted using AllPrep DNA/RNA Kit (Qiagen) following manufacturer's instruction.

The concentration of the RNA extracted was assessed using the Quant-iT™ RNA BR Assay Kit on a Qubit™ Quantitation Platform (ThermoFisher Scientific, Waltham, Massachusetts, USA).

6.2 RETROTRANSCRIPTION AND NEXT GENERATION SEQUENCING PROTOCOL

RNA retrotranscription and NGS were carried out using Ion S5 XL platform (LifeTechnologies), following manufacturer's instruction.

Briefly, 10ng of RNA were reverse transcribed as reported in **Table 9**. Target genes were then amplified using RNA custom panel, following condizione reported in **Table 10**.

<i>Reaction Mix</i>	
Component	Volume (μ l)
5X VILO RT Reaction Mix	2
10X Superscript III Enzyme Mix	1
Total RNA (10ng)	≤ 6
Nuclease-free Water	to 10
<i>Protocol</i>	
Temperature ($^{\circ}$ C)	Time
42	30'
85	5'
4	∞

Table 9. *Reaction mix and steps used for RNA retrotranscription.*

<i>Reaction Mix</i>	
Component	Volume (μ l)
5X Ion AmpliSeq HiFi Mix	4
5X Ion RNA panel	1
Nuclease-free Water	2
RT product	10
<i>Protocol</i>	
Temperature ($^{\circ}$ C)	Time
99	2'
99	15''
60	4'
10	∞

Table 10. *Amplification condition of RT product.*

After a partial digestion of primer sequences with FuPa Reagent, each sample was “barcoded” using Ion P Adapter and Ion Ampliseq Barcode. Barcoded amplicons were purified using a two-round purification, based on the use of magnetic beads.

The library was amplified using reagent and protocol reported in **Table 11**.

<i>Reaction Mix</i>	
Component	Volume (µl)
Platinum PCR SuperMix HiFi	50
Library amplification primer mix	2
Purified library	10
<i>Protocol</i>	
Temperature (°C)	Time
98	2'
98	15''
60	1'
10	≤ 24 hours

Table 11. *Condition used for library amplification.*

Amplified amplicons were then purified and quantified using Quant-iT™ dsDNA HR Assay Kit on a Qubit™ Quantitation Platform (ThermoFisher Scientific). The amplicon library was then diluted to a concentration of approximately 15ng/ml.

The sequencing was then carried out on Ion S5 XL platform.

7 STATISTICAL ANALYSIS

Statistical analysis were performed using the one-way analysis of variance (ANOVA). All tests were completed using Prism (GraphPad, San Diego, CA, USA). A $p < 0.05$ was considered statistically significant. Experiments were carried out at least in duplicates. A mutant (BRAF-G593D) had one replicate.

Results

Aim 1: Detection of BRAF mutations in non-malignant tissue and analysis of BRAF-mutant activity

1 NEXT GENERATION SEQUENCING

Sequencing (NGS) results are summarized in **Table 12**.

1.1 THYROID NEOPLASIA MOLECULAR PROFILE

We analyzed the *BRAF* exon 15 status of 30 thyroid cancers.

Ten out of 30 (33.3%) samples were *BRAF* WT; 5 (50.0%) were PTC-FV, while 5 (50.0%) were PTC-CL.

One sample (PTC-FV) (3.3%) was positive for *BRAF* p.V600A.

In 19 out of 30 samples (63.3%) were detected the *BRAF* p.V600E. Ten out of 19 (52.6%) were PTC-CL, 3 (15.8%) were PTC-FV, while 5 (26.3%) were PTC-TC. One sample (5.3%) was a sclerosing PTC.

1.2 NON-MALIGNANT THYROID TISSUE MOLECULAR PROFILE

We had analyzed 100 non-malignant tissue surrounding the PTCs.

Eighty-five sample (85.0%) out of 100 were *BRAF* WT, while 12 samples (12.0%) were positive for a *BRAF* mutation. Three cases (3.0%) were not evaluable.

Among positive cases, sample 4a (FA-ONC) and sample 12b (HYP) harbored two mutations: p.V600K&p.S607P and p.G593D&p.Q603R, respectively.

Case	Age	Sex	Diagnosis	Result
1			PTC-FV	p.V600E
1a	60	F	ATY	WT
1b			HYP	WT
1c			NORM	WT
2				Sclerosing PTC
2a	45	F	ATY	WT
2b			ATY	WT
2c			NORM	WT
3				PTC-FV
3a	52	F	PsB	p.V600E
3b			NORM	WT
4			PTC-CL	p.V600E
4a	55	F	FA-ONC	p.V600K p.S607P
4b			HYP	p.S607P
4c			NORM	WT
4d			HYP	WT
4e			NORM	WT
4f			FA-ONC	WT
5				
5a	61	F	ATY	WT
5b			NORM	WT
5c			HYP	WT
6				
6a	51	M	ATY	WT
6b			PsB	p.V600E
6c			NORM	WT
6d			HYP	WT
6e			ATY	WT
6f			NORM	WT
7				
7a	36	F	ATY	p.V600M
7b			NORM	WT
7c			NORM	WT
7d			ATY	WT
8				
8a	79	F	PsB	p.V600E
8b			NORM	WT
8d			NORM	p.S607F

Case	Age	Sex	Diagnosis	Result
9			PTC-CL	p.V600E
9a			ATY	WT
9b			HYP	WT
9c	61	M	NORM	WT
9d			HYP	WT
9e			NORM	WT
9f			ATY	WT
10			PTC-TC	p.V600E
10a	30	F	ATY	WT
10b			NORM	WT
11			PTC-CL	p.V600E
11a	49	M	ATY	WT
11b			FA	WT
11c			NORM	WT
12			PTC-CL	p.V600E
12a			ATY	p.G593D
12b			HYP	p.G593D
12c	49	M	NORM	WT
12d			ATY	NE
12e			ATY	WT
12f			NORM	NE
13			PTC-TC	p.V600E
13a			ATY	WT
13b			ATY	WT
13c	35	M	NORM	WT
13d			ATY	p.G593D
13e			HYP	WT
13f			ATY	WT
14			PTC-CL	p.V600E
14 a	49	F	ATY	WT
14 b			NORM	WT
14 c			ATY	WT
15			PTC-CL	p.V600E
15 a	36	M	ATY	WT
15 b			NORM	WT
15 c			ATY	WT
16			PTC-TC	p.V600E
16 a	58	F	NORM	WT
16 b			ATY	p.A598T
16 c			ATY	WT

Case	Age	Sex	Diagnosis	Result
17			PTC-TC	p.V600E
17 a	37	F	ATY	WT
17 b			ATY	WT
17 c			HYP	WT
18				PTC-CL
18 a	32	F	NORM	WT
18 b			ATY	WT
18 c			ATY	WT
19				PTC-CL
19 a	47	F	HYP	WT
19 b			HYP	WT
19 c			ATY	WT
20				PTC-FV
20a	70	F	NORM	WT
20b			HYP	WT
21			PTC-FV	p.V600A
21a	73	F	NORM	WT
21b			ATY	WT
21c			HYP	WT
22				
22a	51	M	NORM	WT
22b			PsB	WT
23			PTC-FV	WT
23a	61	M	NORM	WT
23b			Hyp	WT
24			PTC-FV	WT
24a	32	F	ATY	NE
24b			ATY	WT
24c			PsB	WT
25			PTC-CL	WT
25a	44	M	NORM	WT
25b			ATY	WT
25c			HYP	WT
25d			PsB	WT
26				
26a	33	F	NORM	WT
26b			ATY	WT
27			PTC-FV	WT
27a	30	M	NORM	WT
27b			FA	WT
27c			FA	WT

Case	Age	Sex	Diagnosis	Result
28			PTC-CL	WT
28a	36	F	NORM	WT
28b			NORM	WT
28c			FA	p.K601E
29			PTC-FV	WT
29a	29	F	NORM	WT
29b			ATY	WT
30			PTC-CL	WT
30a	48	F	ATY	WT
30b			ATY	WT
30c			NORM	WT

Table 12: Next Generation Sequencing results.

If only normal thyroid tissues are considered, 34 specimens were analyzed, among which 32 (94.1%) were *BRAF* WT. One out of 34 (2.9%) was not evaluable, while 1 (2.9%) was positive for the mutational calling for p.S607F.

Among hyperplastic tissue, 14 (87.5%) out of 16 samples analyzed were negative for *BRAF* mutation, whereas 2 samples (4b and 12b) (12.5%) were positive for the presence of *BRAF* mutation. We observed p.S607P substitution in sample 4b, while the sample 12b harbored two mutations, p.G593D&p.Q603R.

When only atypical tissue is considered, 38 specimens were analyzed. Thirty-two samples (84.2%) were *BRAF* WT, whereas 2 (5.3%) were not evaluable for *BRAF* status. Four samples (10.5%) harbored a *BRAF* mutation: sample 7a showed p.V600M, 2 samples (12a and 13d) were *BRAF* p.G593D (**Figure 9.B**), and sample 6b was positive for p.A598T.

Six specimens analyzed had psammoma body; 3 (50.0%) were *BRAF* WT, whereas 3 (50.0%) were *BRAF* p.V600E (**Figure 9.A**).

Six FA were analyzed, among which 2 were FA-ONC. We observed 2 mutated sample (33.3%): sample 28c (FA) was positive for p.K601E, whereas sample 4a (FA-ONC) harboured two mutations, p.V600K&p.S607P. Four specimens (66.6%) were *BRAF* WT.

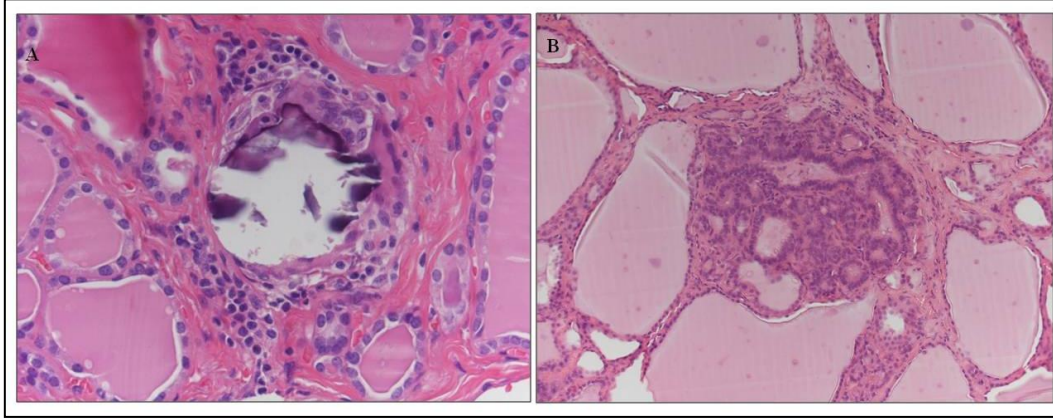


Figure 9: A) tissue containing psammoma body *BRAF* p.V600E (x600); B) atypical thyroid tissue *BRAF* p.G593D positive (x600).

Considering only non-malignant tissue surrounding *BRAF* p.V600E-positive carcinoma, 74 non-malignant specimens were analyzed (**Table 13**). Eleven out of 74 (14.9%) showed a *BRAF* mutation, while 61 (82.4%) were WT. Two samples (2.7%) were not evaluable.

If only non-malignant tissue surrounding *BRAF* WT carcinoma were considered, we analyzed 26 specimens, among which 24 (92.3%) were WT, sample 24a (ATY) (3.8%) was NE and sample 28c (FA) (3.8%) was p.K601E (**Table 13**).

PTC <i>BRAF</i> V600-positive (n=20)			
<i>Non-malignant tissue (n=74)</i>	WT (%)	MUT (%)	NE (%)
ATY (n=31)	26 (83.9%)	4 (12.9%)	1 (3.2%)
HYP (n=13)	11 (84.6%)	2 (15.4%)	-
NORM (n=24)	22 (91.7%)	1 (4.2%)	1 (4.2%)
PsB (n=3)	-	3 (100.0%)	-
FA-ONC (n=2)	1 (50.0%)	1 (50.0%)	-
FA (n=1)	1 (100.0%)	-	-
PTC <i>BRAF</i> WT (n=10)			
<i>Non-malignant tissue (n=26)</i>	WT (%)	MUT (%)	NE (%)
ATY (n=7)	6 (85.7%)	-	1 (14.3%)
HYP (n=3)	3 (100.0%)	-	-
NORM (n=10)	10 (100.0%)	-	-
PsB (n=3)	3 (100,0%)	-	-
FA (n=3)	2 (66,7%)	1 (33,3%)	-

Table 13: Comparison between *BRAF*-V600 positive and *BRAF* WT tumors

In order to understand the possible impact of “uncommon” alterations found in non-malignant tissue, the tool PolyPhen-2 (Polymorphism Phenotyping v2) was used. PolyPhen-2 is an *in silico* tool that predicts if a mutation could be benign (B, score: 0-0.2), possibly damaging (PoD, score: 0.2-0.85) or probably damaging (PD, score: 0.85-1.00). All the mutations observed are reported in **Table 14**.

Non-malignant tissue (n)	Mutation	Reference (PMID)	PolyPhen (score)
ATY (2), HYP (1)	p.G593D	PMID: 19269016	PD (1.000)
ATY	p.A598T	PMID: 22926515	PD (0.871)
PsB (3),	p.V600E	PMID: 15035987	PD (0.971)
*FA-ONC (1)	p.V600K	PMID: 15035987	PD (1.000)
ATY (1)	p.V600M	PMID: 28783719	PD (0.904)
FA(1)	p.K601E	PMID: 15035987	PoD (0.784)
HYP (1)	p.R603Q	PMID: 23861977	PoD (0.786)
NORM (1)	p.S607F	PMID: 23861977	PD (0.998)
*FA-ONC (1), HYP (1)	p.S607P	PMID: 29176861	B (0.186)

Table 14: Mutation found in non-malignant tissue surrounding the PTC. “Uncommon” BRAF mutations other than p.V600E or p.K601E are present in 9 samples: * one sample, FA-ONC harboured two mutations (p.V600K and p.S607P).

2 FUNCTIONAL CHARACTERIZATION OF *BRAF* MUTATIONS

2.1 SELECTION OF MUTANT TO TEST

To comprehend if the “uncommon” *BRAF* alteration affects the protein activity, we decided to investigate mutations p.G593D, p.A598T, p.S607F, p.S607P found in non-malignant tissue surrounding carcinoma.

We compared BRAF mutant activity to the WT protein and to those with a increased activity (p.V600E, p.K601E).

2.2 FUNCTIONAL CHARACTERIZATION

Through the MAPK pathway, BRAF phosphorylates MEK1/2 at serine 217 and 221, and in turn MEK1/2 phosphorylates ERK1/2 at threonine 202 and tyrosine 204. We transiently expressed BRAF-G593D, BRAF-A598T, BRAF-S607F, BRAF-S607P, BRAF-V600E, BRAF-K601E (both known to lead to a higher protein activity) mutant and BRAF-WT in HEK293 cells. Forty-eight hours after cell transfection, total proteins were extracted and immunoblotting was carried out. We evaluated the phosphorylation level of the protein involved in MAPK pathway (ERK1/2, MEK1/2, BRAF) using specific antibodies.

Densitometric analysis result have been normalized to non-transfected control.

Phosphorylation level of ERK1/2 was higher in BRAF-V600E (3.8 fold) and in BRAF-K601E (2.7 fold) when compared to BRAF-WT ($p < 0.05$). In BRAF-G593D and BRAF-A598T ERK1/2 phosphorylation level was lower than BRAF-WT, but it was not statistically significant. Phosphorylation level of ERK1/2 in BRAF-S607F and BRAF-S607P was similar to BRAF-WT (**Figure 10**).

Phosphorylation levels of MEK1/2 show a similar trend to those of ERK1/2: p-MEK1/2 was higher in BRAF-V600E (3.3 fold) and in BRAF-K601E (3.3 fold) when compared to BRAF-WT, but it was not statistically significant. In BRAF-G593D and BRAF-A598T MEK1/2 phosphorylation level was lower than BRAF-WT, but it was not statistically significant. Phosphorylation level of MEK1/2 in BRAF-S607F and BRAF-S607P was similar to BRAF-WT (**Figure 10**).

BRAF phosphorylation level in BRAF-G593D, BRAF-A598T, BRAF-V600E, BRAF-K601E, BRAF-S607F and BRAF-S607P was similar to BRAF-WT (**Figure 10**).

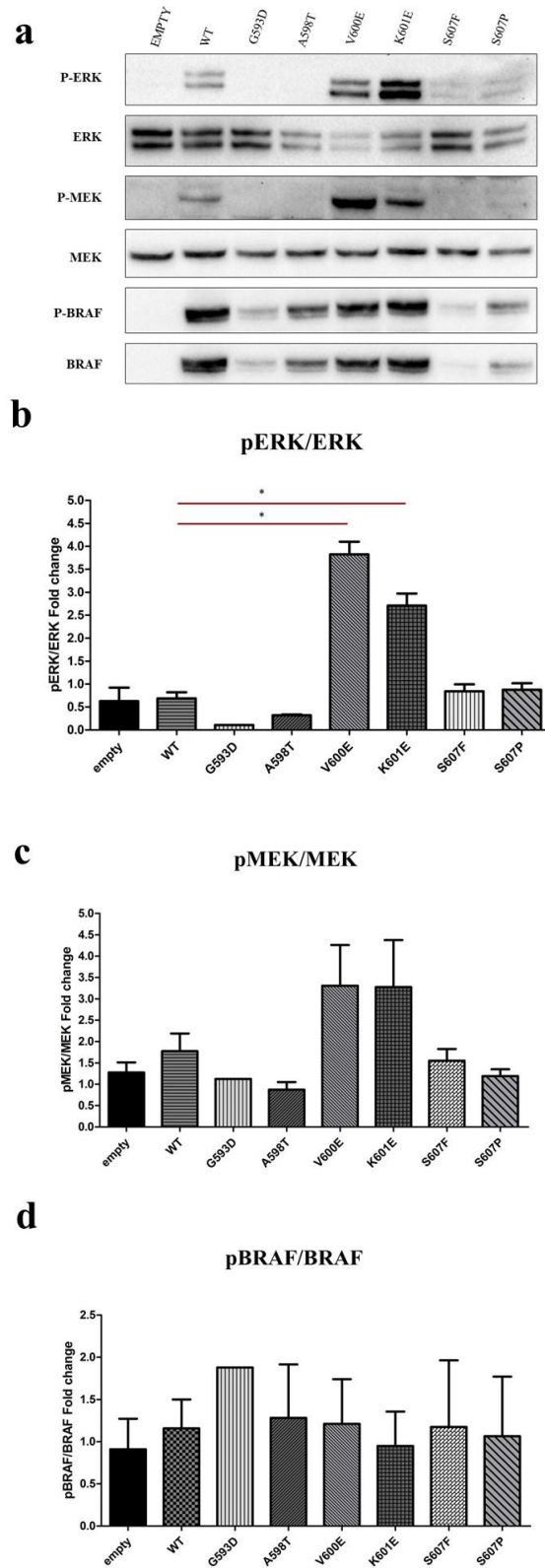


Figure 10: Functional characterization of the *BRAF-G593D*, *BRAF-A598T*, *BRAF-S607F*, *BRAF-S607P*. (a) Effect of BRAF mutants on the MAPK signaling pathway. (b) Effect of BRAF mutants on the ERK1/2 phosphorylation level. (c) Effect of BRAF mutants on the MEK1/2 phosphorylation level. (d) Effect of BRAF mutants on the BRAF phosphorylation level.

Aim 2: Design and set up of a gene expression panel.

3 GENE PANEL RESULTS

We designed an expression gene panel, which included gene fusions, biomarker and thyroid lineage and differentiation, genes involved in immune-oncology, genes involved in BRAF-like or RAS-like profiling, genes up/down regulated in cancers and proliferation genes.

DNA and RNA were extracted from 44 FF specimens, RNA was retrotranscribed and NGS analysis was carried out. In **Figure 11** is reported the heatmap, obtained from an unsupervised hierarchical cluster analysis.

In our panel, we included genes known to be differentially expressed in *BRAF*-positive carcinoma (*BRAF*-like signature) or in *RAS*-positive sample (*RAS*-like signature) (**Supplementary Table 1**).

If only *BRAF*-like signature genes are considered, they show an over-expression in PTCs-TC, PTCs-CL. Intriguingly, *BRAF*-like signature genes were over-expressed in sample Thy101 (PTC-FV): previous molecular analysis showed Thy101 to harbor a mutation in *BRAF* exon 15. *BRAF*-like genes were down-regulated in non-malignant sample and *RAS*-positive specimens (PTC-FV, FTC). Under-expression was observed in HCC. In Thy001, Thy182-2 *BRAF*-positive (ATCs) *BRAF*-like signature genes were not over-expressed.

Similarly, *RAS*-like signature genes are over-expressed in *RAS*-positive samples (PTC-FV, FA, FTC).

We analyzed the expression of 38 genes involved in cell proliferation, such as *EZH2* or *PBK*. They result over-expressed in *BRAF*-positive samples including PTCs-TC and PTCs-CL. Differently from *BRAF*-like signature genes, cell proliferation genes were over-expressed ATCs, both *BRAF*-positive (Thy001 and Thy182-2) and WT (Thy022).

The expression of 16 genes involved in thyroid differentiation and biomarker for thyroid lineage was analyzed. They result under-regulated in 2 ATC *BRAF*-positive (Thy001 and Thy182-2), in CRC and in MTC. Differently

from Thy001 and Thy182-2, Thy022 (ATCs) had the same expression pattern of well-differentiated cancers. The expression of biomarker genes was over-regulated in normal, hyperplastic and non-malignant tissue (including FAs), in FTC BRAF-WT, and in 2 *RAS*-positive PTCs-FV (Thy132 and Thy135).

In 3 FTCs (Thy085, Thy093, Thy121) were confirmed the *PAX8/PPARG* rearrangement, a marker for follicular patterned cancers.

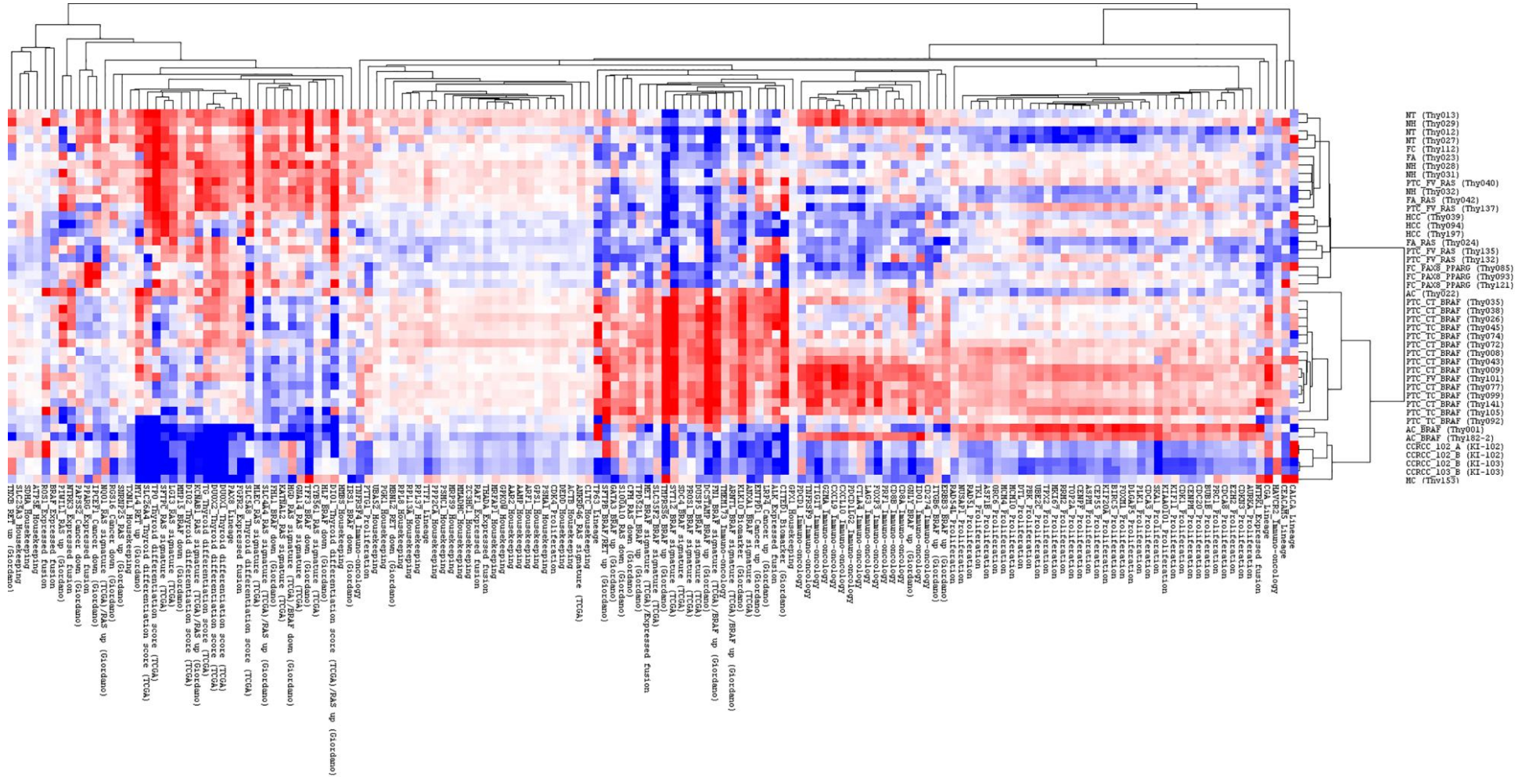


Figure 11: Heatmap obtained from an unsupervised hierarchical cluster analysis.

Discussion

Aim 1: Detection of BRAF mutations in non-malignant tissue and analysis of BRAF-mutant activity

Papillary carcinoma is one the most well characterized cancer, and its molecular signature has been deeply investigated [64]. *BRAF* alterations are the most frequent driver mutations in thyroid cancers (40-45%), and the ~95% are represented the *BRAF* p.V600E substitution, which mimics the protein phosphorylation and results in its the constitutive activation [20, 83, 107]. To date, there are no information regarding the *BRAF* molecular profile of the non-malignant tissue surrounding the carcinoma. Exploring the *BRAF* molecular signature of tissue surrounding carcinomas could be helpful to better understand the thyroid tumorigenesis and the events that lead the precursor lesions to evolve, or not, to carcinoma.

In this study, we explored the *BRAF* status of 100 areas of non-malignant tissue surrounding 10 PTCs *BRAF* WT and 20 PTCs *BRAF*-positive. Intriguingly, no mutations were found in all tissues but one surrounding *BRAF*-WT carcinomas. In one FA adjacent a *BRAF*-WT PTC a *BRAF* p.K601E alteration was found. This data is not surprising, in fact, p.K601E is known to be associated with follicular-pattern alteration in thyroid neoplasms, and it leads to a better outcome than p.V600E positive nodules. Specifically, p.K601E mutation has been also previously described in FA tumor [114].

In non-malignant tissue surrounding *BRAF* positive PTCs we found “common” mutations (in codons 600) in areas containing psammoma body (p.V600E), oncocytic follicular adenoma (p.V600K) or with an atypical architecture (p.V600M).

The *BRAF* p.V600E mutation was found in areas containing psammoma bodies (PsB). PsB are considered to be the “the ghosts of dead papillae”:

they are calcifications resulting from a progressive depositum of calcium on dying cells, that confer them a characteristic lamellation [181-183], and could arise from nests of tumor cells, as demonstrated by Johannessen and colleagues [182]. Finding the BRAF p.V600E mutation in PsB surrounding BRAF-V600E PTC is a further evidence that PsB are a footprint of “dead” neoplastic cells.

The *BRAF* p.V600K mutation was recently characterized for conferring a gain of function to the BRAF protein, resulting in an increased kinase activity [184]. We found *BRAF* p.V600K mutation in an oncocytic follicular adenoma, arising in a BRAF p.V600E context. Considering that p.V600E mutation is a c.1799T>A substitution, we supposed that a second point mutation occurred in c.1798G>A residue, resulting in c.1798-1799GT>AA (p.V600K) alteration.

The *BRAF* p.V600M mutation was detected in an area with an atypical architecture. It is conceivable that this area was transforming into a neoplastic one. In fact, p.V600M mutation was previously reported to have an intermediate kinase activity (lower than BRAF-V600E protein but higher than BRAF-WT one) in cell culture [184].

The following “uncommon” mutations (different from codon 600) were found in *BRAF* exon 15: p.G593D, p.A598T, p.R603Q, p.S607F and p.S607P. All of them were previously reported in literature and described in different neoplastic tissue. The p.G593D was found in solid cell nest hyperplasia associated with BRAF p.V600E papillary thyroid carcinoma [185].

Both p.R603Q and p.S607F mutations were reported in nevi, in association with *BRAF*-positive melanoma [186], similarly to what we observed in our non-malignant area surrounding BRAF-V600E PTC.

The p.S607P substitution was previously described in melanoma [187], while the p.A598T were detected in non small cell lung cancers [188] and correlates with a decreased activity of BRAF protein [189].

All “uncommon” BRAF mutations were observed in non-malignant tissues surrounding *BRAF*-positive PTCs, while they were not detected in tissues surrounding the BRAF-WT carcinomas. The higher frequency of this

uncommon mutation in non-malignant tissue surrounding *BRAF*-positive PTCs could be due to a genomic instability. Mitmaker and colleagues analyzed for microsatellite instability (MSI) both benign and malignant thyroid neoplasms, comparing them to adjacent normal tissue. They demonstrated a high rate of MSI both in FTC and PTC (9/14 and 10/16 sample analyzed, respectively), while benign follicular adenomas showed no genomic instability or had a low-MSI [190]. On the contrary, Nikiforov and colleagues showed that MSI does not seem to contribute to thyroid carcinogenesis, especially in radiation-induced thyroid cancer [191]. Further studies are necessary in order to clarify the possible link between MSI and presence of “uncommon” mutations in thyroid carcinogenesis.

Through the MAPK pathway, BRAF protein phosphorylates MEK1/2 in turn MEK1/2 phosphorylates ERK1/2. We transiently expressed BRAF-G593D, BRAF-A598T, BRAF-V600E, BRAF-K601E, BRAF-S607F and BRAF-S607P mutant, the phosphorylation levels of ERK1/2, MEK1/2 and BRAF proteins were assessed.

“Uncommon” BRAF mutants analyzed (BRAF-G593D, BRAF-A598T, BRAF-S607F and BRAF-S607P) were not associated with an increased MAPK pathway activation. On the contrary, they seemed to have the same (or lower) activation of MAPK pathway if compared to BRAF-WT protein. In particular, BRAF-G53D and BRAF-A598T seemed to have a lower BRAF activity.

We compared the activity of BRAF mutant found in non-malignant tissue (BRAF-G593D, BRAF-A598T, BRAF-S607F and BRAF-S607P) to the one of BRAF-WT, BRAF-V600E and BRAF-K601E proteins. As expected, we observed higher level of activation of MAPK pathway in BRAF-V600E and BRAF-K601E when compared to WT. In fact, it is well known that these alterations lead to a constitutive activation of BRAF protein [102].

BRAF phosphorylation level of BRAF-G593D, BRAF-A598T, BRAF-V600E, BRAF-K601E, BRAF-S607F and BRAF-S607P were similar to BRAF-WT. As expected, both “common” and “uncommon” *BRAF* mutations do not lead to an increase phosphorylation level of the protein. In

fact, activating mutations, such as p.V600E and p.K601E, mimic the phosphorylation of the activation segment, but they do not increase the BRAF affinity for the phosphate [102].

BRAF p.G593D and p.A598T mutants showed a lower MAPK pathway activation when compared to BRAF WT. These results are comparable with those obtained by Rebocho and colleagues [189]. Alterations in histological architecture in tissue harbouring these mutations could be due to other defects in genes involved in cell proliferation, such as *RAS* or PI3K/AKT/PTEN pathway. Exploring the molecular signature of oncogenes different from *BRAF*, such as *RAS*, could clarify the development of histologically benign thyroid lesions.

Aim 2: Design and set up of a gene expression panel.

The combination of cytology analysis and molecular testing have improved the pre-operative evaluation of thyroid lesions. However, a lot of pre-operative samples are diagnosed as “indeterminate” (Thy-3 according to cytological classification of thyroid samples). Understanding the molecular expression assessment in thyroid lesions could be useful for the establishment of a correct surgical approach, as well as treatment decision and prognostic information.

The expression panel was designed to detect gene fusion and gene expression recurrently altered in thyroid cancers and with potential for diagnostic and clinical relevance. We verified that our panel is able to clusterize sample in three main groups: i) non-malignant tissue; ii) malignant tissue; iii) non-follicular thyroid cell derived cancers.

We analyzed the expression of genes involve in thyroid differentiation and lineage, observing an up-regulation in non-malignant samples, including normal and hyperplastic tissue and follicular adenoma. A down-regulation was observed in two ATCs (Thy001 and Thy182-2), in CRC and in MTC. The expression level of these gene could be very useful for clusterization in

non-malignant *versus* malignant tissue. Considering non-malignant tissue cluster, we observed three outlier samples: in fact, Thy112 (FTC), Thy040 and Thy137 (both PTC-FV) had the same expression pattern of non-malignant specimens. On the contrary, a *RAS*-positive FA (Thy024) was clusterized as malignant. Differently from Thy001 and Thy182-2, Thy022 (ATC) had the same expression pattern of well-differentiated cancers. The expression level analysis of these genes is able to well clusterized non-malignant sample, undifferentiated carcinoma, and non-follicular thyroid cells derived cancer from follicular cells derived malignant neoplasia.

In our panel, we included genes known to be differentially expressed in *BRAF*-positive carcinoma (*BRAF*-like signature) or in *RAS*-positive sample (*RAS*-like signature). When only malignant tissue is considered, our panel is able to clusterize sample in to follicular patterned cancer and papillary patterned cancer. Intriguingly, Thy101 (PTC-FV *BRAF*-positive) was clusterized as a *BRAF*-like sample, even if it had a follicular pattern histological architecture.

In our panel, primers were design to detect known recurrent gene fusions (through primers annealing to the well-known breakpoint) as well as fusions of novel isoforms of *ALK*, *BRAF*, *FGFR2*, *NTRK1*, *NTRK3*, *PPARG*, *RAF1*, *ROS1* and *THADA* genes, through 3'/5' expression imbalance. Furthermore, we confirmed the *PAX8/PPARG* rearrangement in 3 samples.

Further analyses are needed for additional validation and assessment of our gene expression panel.

References

1. Mohebati, A. and A.R. Shaha, *Anatomy of thyroid and parathyroid glands and neurovascular relations*. Clin Anat, 2012. **25**(1): p. 19-31.
2. Nussey, S. and S. Whitehead, in *Endocrinology: An Integrated Approach* 2001: Oxford.
3. N, S., *Anatomy and Physiology of the Thyroid Gland: Clinical Correlates to Thyroid Cancer* 2016.
4. Jemal, A., et al., *Global cancer statistics*. CA Cancer J Clin, 2011. **61**(2): p. 69-90.
5. Ito, Y., et al., *Increasing incidence of thyroid cancer: controversies explored*. Nat Rev Endocrinol, 2013. **9**(3): p. 178-84.
6. Xing, M., *Molecular pathogenesis and mechanisms of thyroid cancer*. Nat Rev Cancer, 2013. **13**(3): p. 184-99.
7. Fagin, J.A. and S.A. Wells, Jr., *Biologic and Clinical Perspectives on Thyroid Cancer*. N Engl J Med, 2016. **375**(23): p. 2307.
8. McHenry, C.R. and R. Phitayakorn, *Follicular adenoma and carcinoma of the thyroid gland*. Oncologist, 2011. **16**(5): p. 585-93.
9. Suster, S., *Thyroid tumors with a follicular growth pattern: problems in differential diagnosis*. Arch Pathol Lab Med, 2006. **130**(7): p. 984-8.
10. Lloyd, R.V.O., Robert Y; Klöppel, Günter; Rosai, Juan, *WHO classification of tumours of endocrine organs* 4th edition ed, ed. W.H.O.I.A.f.R.o. Cancer 2017.
11. Davies, L. and H.G. Welch, *Current thyroid cancer trends in the United States*. JAMA Otolaryngol Head Neck Surg, 2014. **140**(4): p. 317-22.
12. Shi, X., et al., *Differential Clinicopathological Risk and Prognosis of Major Papillary Thyroid Cancer Variants*. J Clin Endocrinol Metab, 2016. **101**(1): p. 264-74.
13. Tang, W., et al., *Parathyroid gland involvement by papillary carcinoma of the thyroid gland*. Arch Pathol Lab Med, 2002. **126**(12): p. 1511-4.
14. Okayasu, I., et al., *Association of chronic lymphocytic thyroiditis and thyroid papillary carcinoma. A study of surgical cases among Japanese, and white and African Americans*. Cancer, 1995. **76**(11): p. 2312-8.
15. Kazakov, V.S., E.P. Demidchik, and L.N. Astakhova, *Thyroid cancer after Chernobyl*. Nature, 1992. **359**(6390): p. 21.
16. Williams, D., *Cancer after nuclear fallout: lessons from the Chernobyl accident*. Nat Rev Cancer, 2002. **2**(7): p. 543-9.
17. Ron, E., et al., *Thyroid cancer after exposure to external radiation: a pooled analysis of seven studies*. Radiat Res, 1995. **141**(3): p. 259-77.
18. Iyama, K., et al., *Identification of Three Novel Fusion Oncogenes, SQSTM1/NTRK3, AFAP1L2/RET, and PPFIBP2/RET, in Thyroid Cancers of Young Patients in Fukushima*. Thyroid, 2017. **27**(6): p. 811-818.
19. Ito, Y., et al., *Biological behavior and prognosis of familial papillary thyroid carcinoma*. Surgery, 2009. **145**(1): p. 100-5.
20. Nikiforov, Y.E. and M.N. Nikiforova, *Molecular genetics and diagnosis of thyroid cancer*. Nat Rev Endocrinol, 2011. **7**(10): p. 569-80.
21. Kondo, T., S. Ezzat, and S.L. Asa, *Pathogenetic mechanisms in thyroid follicular-cell neoplasia*. Nat Rev Cancer, 2006. **6**(4): p. 292-306.
22. DeGroot, L.J., et al., *Morbidity and mortality in follicular thyroid cancer*. J Clin Endocrinol Metab, 1995. **80**(10): p. 2946-53.

23. Brennan, M.D., et al., *Follicular thyroid cancer treated at the Mayo Clinic, 1946 through 1970: initial manifestations, pathologic findings, therapy, and outcome*. Mayo Clin Proc, 1991. **66**(1): p. 11-22.
24. Hundahl, S.A., et al., *A National Cancer Data Base report on 53,856 cases of thyroid carcinoma treated in the U.S., 1985-1995 [see commetns]*. Cancer, 1998. **83**(12): p. 2638-48.
25. Tallini, G., *Oncocytic tumours*. Virchows Arch, 1998. **433**(1): p. 5-12.
26. Volante, M., et al., *Poorly differentiated thyroid carcinoma: the Turin proposal for the use of uniform diagnostic criteria and an algorithmic diagnostic approach*. Am J Surg Pathol, 2007. **31**(8): p. 1256-64.
27. Setia, N. and J.A. Barletta, *Poorly Differentiated Thyroid Carcinoma*. Surg Pathol Clin, 2014. **7**(4): p. 475-89.
28. Asioli, S., et al., *Poorly differentiated carcinoma of the thyroid: validation of the Turin proposal and analysis of IMP3 expression*. Mod Pathol, 2010. **23**(9): p. 1269-78.
29. Ito, Y., et al., *Prevalence and prognostic significance of poor differentiation and tall cell variant in papillary carcinoma in Japan*. World J Surg, 2008. **32**(7): p. 1535-43; discussion 1544-5.
30. LiVolsi, V.A., et al., *The Chernobyl thyroid cancer experience: pathology*. Clin Oncol (R Coll Radiol), 2011. **23**(4): p. 261-7.
31. Kebebew, E., et al., *Anaplastic thyroid carcinoma. Treatment outcome and prognostic factors*. Cancer, 2005. **103**(7): p. 1330-5.
32. Moretti, F., et al., *p53 re-expression inhibits proliferation and restores differentiation of human thyroid anaplastic carcinoma cells*. Oncogene, 1997. **14**(6): p. 729-40.
33. Smallridge, R.C., et al., *American Thyroid Association guidelines for management of patients with anaplastic thyroid cancer*. Thyroid, 2012. **22**(11): p. 1104-39.
34. Maatouk, J., et al., *Anaplastic thyroid carcinoma arising in long-standing multinodular goiter following radioactive iodine therapy: report of a case diagnosed by fine needle aspiration*. Acta Cytol, 2009. **53**(5): p. 581-3.
35. Aldinger, K.A., et al., *Anaplastic carcinoma of the thyroid: a review of 84 cases of spindle and giant cell carcinoma of the thyroid*. Cancer, 1978. **41**(6): p. 2267-75.
36. Giordano, T.J., et al., *Molecular classification of papillary thyroid carcinoma: distinct BRAF, RAS, and RET/PTC mutation-specific gene expression profiles discovered by DNA microarray analysis*. Oncogene, 2005. **24**(44): p. 6646-56.
37. Acquaviva, G., et al., *Molecular pathology of thyroid tumours of follicular cells: a review of genetic alterations and their clinicopathological relevance*. Histopathology, 2018. **72**(1): p. 6-31.
38. Farid, N.R. and M.W. Szkudlinski, *Minireview: structural and functional evolution of the thyrotropin receptor*. Endocrinology, 2004. **145**(9): p. 4048-57.
39. Lyons, J., et al., *Two G protein oncogenes in human endocrine tumors*. Science, 1990. **249**(4969): p. 655-9.
40. O'Sullivan, C., et al., *Activating point mutations of the gsp oncogene in human thyroid adenomas*. Mol Carcinog, 1991. **4**(5): p. 345-9.
41. Krohn, K., et al., *Molecular pathogenesis of euthyroid and toxic multinodular goiter*. Endocr Rev, 2005. **26**(4): p. 504-24.
42. Parma, J., et al., *Somatic mutations in the thyrotropin receptor gene cause hyperfunctioning thyroid adenomas*. Nature, 1993. **365**(6447): p. 649-51.
43. Parma, J., et al., *Diversity and prevalence of somatic mutations in the thyrotropin receptor and Gs alpha genes as a cause of toxic thyroid adenomas*. J Clin Endocrinol Metab, 1997. **82**(8): p. 2695-701.

44. Duprez, L., et al., *Germline mutations in the thyrotropin receptor gene cause non-autoimmune autosomal dominant hyperthyroidism*. Nat Genet, 1994. **7**(3): p. 396-401.
45. McCain, J., *The MAPK (ERK) Pathway: Investigational Combinations for the Treatment Of BRAF-Mutated Metastatic Melanoma*. P T, 2013. **38**(2): p. 96-108.
46. Chang, L. and M. Karin, *Mammalian MAP kinase signalling cascades*. Nature, 2001. **410**(6824): p. 37-40.
47. Pearson, G., et al., *Mitogen-activated protein (MAP) kinase pathways: regulation and physiological functions*. Endocr Rev, 2001. **22**(2): p. 153-83.
48. Dong, C., R.J. Davis, and R.A. Flavell, *MAP kinases in the immune response*. Annu Rev Immunol, 2002. **20**: p. 55-72.
49. Soares, P., et al., *BRAF mutations and RET/PTC rearrangements are alternative events in the etiopathogenesis of PTC*. Oncogene, 2003. **22**(29): p. 4578-80.
50. Tanaka, K., et al., *Expression profile of receptor-type protein tyrosine kinase genes in the human thyroid*. Endocrinology, 1998. **139**(3): p. 852-8.
51. Takahashi, M., et al., *Cloning and expression of the ret proto-oncogene encoding a tyrosine kinase with two potential transmembrane domains*. Oncogene, 1988. **3**(5): p. 571-8.
52. Ichihara, M., Y. Murakumo, and M. Takahashi, *RET and neuroendocrine tumors*. Cancer Lett, 2004. **204**(2): p. 197-211.
53. Lai, A.Z., T.S. Gujral, and L.M. Mulligan, *RET signaling in endocrine tumors: delving deeper into molecular mechanisms*. Endocr Pathol, 2007. **18**(2): p. 57-67.
54. Pachnis, V., B. Mankoo, and F. Costantini, *Expression of the c-ret proto-oncogene during mouse embryogenesis*. Development, 1993. **119**(4): p. 1005-17.
55. Plaza-Menacho, I., *Structure and function of RET in multiple endocrine neoplasia type 2*. Endocr Relat Cancer, 2018. **25**(2): p. T79-T90.
56. Mohammadi, M. and M. Hedayati, *A Brief Review on The Molecular Basis of Medullary Thyroid Carcinoma*. Cell J, 2017. **18**(4): p. 485-492.
57. de Groot, J.W., et al., *RET as a diagnostic and therapeutic target in sporadic and hereditary endocrine tumors*. Endocr Rev, 2006. **27**(5): p. 535-60.
58. Schilling, T., et al., *Prognostic value of codon 918 (ATG-->ACG) RET proto-oncogene mutations in sporadic medullary thyroid carcinoma*. Int J Cancer, 2001. **95**(1): p. 62-6.
59. Elisei, R., et al., *Prognostic significance of somatic RET oncogene mutations in sporadic medullary thyroid cancer: a 10-year follow-up study*. J Clin Endocrinol Metab, 2008. **93**(3): p. 682-7.
60. Grieco, M., et al., *PTC is a novel rearranged form of the ret proto-oncogene and is frequently detected in vivo in human thyroid papillary carcinomas*. Cell, 1990. **60**(4): p. 557-63.
61. Klugbauer, S., et al., *Detection of a novel type of RET rearrangement (PTC5) in thyroid carcinomas after Chernobyl and analysis of the involved RET-fused gene RFG5*. Cancer Res, 1998. **58**(2): p. 198-203.
62. Ciampi, R., et al., *HOOK3-RET: a novel type of RET/PTC rearrangement in papillary thyroid carcinoma*. Endocr Relat Cancer, 2007. **14**(2): p. 445-52.
63. Stransky, N., et al., *The landscape of kinase fusions in cancer*. Nat Commun, 2014. **5**: p. 4846.
64. *Integrated genomic characterization of papillary thyroid carcinoma*. Cell, 2014. **159**(3): p. 676-90.

65. Corvi, R., et al., *RET/PCM-1: a novel fusion gene in papillary thyroid carcinoma*. *Oncogene*, 2000. **19**(37): p. 4236-42.
66. Bongarzone, I., et al., *Molecular characterization of a thyroid tumor-specific transforming sequence formed by the fusion of ret tyrosine kinase and the regulatory subunit RI alpha of cyclic AMP-dependent protein kinase A*. *Mol Cell Biol*, 1993. **13**(1): p. 358-66.
67. Klugbauer, S. and H.M. Rabes, *The transcription coactivator HTIF1 and a related protein are fused to the RET receptor tyrosine kinase in childhood papillary thyroid carcinomas*. *Oncogene*, 1999. **18**(30): p. 4388-93.
68. Pozdeyev, N., et al., *Genetic Analysis of 779 Advanced Differentiated and Anaplastic Thyroid Cancers*. *Clin Cancer Res*, 2018. **24**(13): p. 3059-3068.
69. Viola, D., et al., *KIF5B/RET Rearrangement in a Carcinoma of the Thyroid Gland: A Case Report of a Fatal Disease*. *J Clin Endocrinol Metab*, 2017. **102**(9): p. 3091-3096.
70. Salassidis, K., et al., *Translocation t(10;14)(q11.2;q22.1) fusing the kinetin to the RET gene creates a novel rearranged form (PTC8) of the RET proto-oncogene in radiation-induced childhood papillary thyroid carcinoma*. *Cancer Res*, 2000. **60**(11): p. 2786-9.
71. Adeniran, A.J., et al., *Correlation between genetic alterations and microscopic features, clinical manifestations, and prognostic characteristics of thyroid papillary carcinomas*. *Am J Surg Pathol*, 2006. **30**(2): p. 216-22.
72. Tallini, G. and S.L. Asa, *RET oncogene activation in papillary thyroid carcinoma*. *Adv Anat Pathol*, 2001. **8**(6): p. 345-54.
73. Smida, J., et al., *Distinct frequency of ret rearrangements in papillary thyroid carcinomas of children and adults from Belarus*. *Int J Cancer*, 1999. **80**(1): p. 32-8.
74. Nikiforov, Y.E., et al., *Distinct pattern of ret oncogene rearrangements in morphological variants of radiation-induced and sporadic thyroid papillary carcinomas in children*. *Cancer Res*, 1997. **57**(9): p. 1690-4.
75. Nakagawara, A., *Trk receptor tyrosine kinases: a bridge between cancer and neural development*. *Cancer Lett*, 2001. **169**(2): p. 107-14.
76. Martin-Zanca, D., S.H. Hughes, and M. Barbacid, *A human oncogene formed by the fusion of truncated tropomyosin and protein tyrosine kinase sequences*. *Nature*, 1986. **319**(6056): p. 743-8.
77. Rabes, H.M., et al., *Pattern of radiation-induced RET and NTRK1 rearrangements in 191 post-chernobyl papillary thyroid carcinomas: biological, phenotypic, and clinical implications*. *Clin Cancer Res*, 2000. **6**(3): p. 1093-103.
78. Prasad, M.L., et al., *NTRK fusion oncogenes in pediatric papillary thyroid carcinoma in northeast United States*. *Cancer*, 2016. **122**(7): p. 1097-107.
79. Bongarzone, I., et al., *RET/NTRK1 rearrangements in thyroid gland tumors of the papillary carcinoma family: correlation with clinicopathological features*. *Clin Cancer Res*, 1998. **4**(1): p. 223-8.
80. Musholt, T.J., et al., *Prognostic significance of RET and NTRK1 rearrangements in sporadic papillary thyroid carcinoma*. *Surgery*, 2000. **128**(6): p. 984-93.
81. Butti, M.G., et al., *A sequence analysis of the genomic regions involved in the rearrangements between TPM3 and NTRK1 genes producing TRK oncogenes in papillary thyroid carcinomas*. *Genomics*, 1995. **28**(1): p. 15-24.
82. Greco, A., et al., *Chromosome 1 rearrangements involving the genes TPR and NTRK1 produce structurally different thyroid-specific TRK oncogenes*. *Genes Chromosomes Cancer*, 1997. **19**(2): p. 112-23.

83. Radice, P., et al., *The human tropomyosin gene involved in the generation of the TRK oncogene maps to chromosome 1q31*. *Oncogene*, 1991. **6**(11): p. 2145-8.
84. Greco, A., et al., *TRK-T1 is a novel oncogene formed by the fusion of TPR and TRK genes in human papillary thyroid carcinomas*. *Oncogene*, 1992. **7**(2): p. 237-42.
85. Greco, A., et al., *The DNA rearrangement that generates the TRK-T3 oncogene involves a novel gene on chromosome 3 whose product has a potential coiled-coil domain*. *Mol Cell Biol*, 1995. **15**(11): p. 6118-27.
86. Pierotti, M.A., *Chromosomal rearrangements in thyroid carcinomas: a recombination or death dilemma*. *Cancer Lett*, 2001. **166**(1): p. 1-7.
87. Leeman-Neill, R.J., et al., *ETV6-NTRK3 is a common chromosomal rearrangement in radiation-associated thyroid cancer*. *Cancer*, 2014. **120**(6): p. 799-807.
88. Ricarte-Filho, J.C., et al., *Identification of kinase fusion oncogenes in post-Chernobyl radiation-induced thyroid cancers*. *J Clin Invest*, 2013. **123**(11): p. 4935-44.
89. Iwahara, T., et al., *Molecular characterization of ALK, a receptor tyrosine kinase expressed specifically in the nervous system*. *Oncogene*, 1997. **14**(4): p. 439-49.
90. Morris, S.W., et al., *Fusion of a kinase gene, ALK, to a nucleolar protein gene, NPM, in non-Hodgkin's lymphoma*. *Science*, 1995. **267**(5196): p. 316-7.
91. Marino-Enriquez, A. and P. Dal Cin, *ALK as a paradigm of oncogenic promiscuity: different mechanisms of activation and different fusion partners drive tumors of different lineages*. *Cancer Genet*, 2013. **206**(11): p. 357-73.
92. Chiarle, R., et al., *The anaplastic lymphoma kinase in the pathogenesis of cancer*. *Nat Rev Cancer*, 2008. **8**(1): p. 11-23.
93. Palmer, R.H., et al., *Anaplastic lymphoma kinase: signalling in development and disease*. *Biochem J*, 2009. **420**(3): p. 345-61.
94. Hamatani, K., et al., *Rearranged anaplastic lymphoma kinase (ALK) gene in adult-onset papillary thyroid cancer amongst atomic bomb survivors*. *Thyroid*, 2012. **22**(11): p. 1153-9.
95. Kelly, L.M., et al., *Identification of the transforming STRN-ALK fusion as a potential therapeutic target in the aggressive forms of thyroid cancer*. *Proc Natl Acad Sci U S A*, 2014. **111**(11): p. 4233-8.
96. Perot, G., et al., *Identification of a recurrent STRN/ALK fusion in thyroid carcinomas*. *PLoS One*, 2014. **9**(1): p. e87170.
97. Landa, I., et al., *Genomic and transcriptomic hallmarks of poorly differentiated and anaplastic thyroid cancers*. *J Clin Invest*, 2016. **126**(3): p. 1052-66.
98. Chou, A., et al., *A detailed clinicopathologic study of ALK-translocated papillary thyroid carcinoma*. *Am J Surg Pathol*, 2015. **39**(5): p. 652-9.
99. Marais, R. and C.J. Marshall, *Control of the ERK MAP kinase cascade by Ras and Raf*. *Cancer Surv*, 1996. **27**: p. 101-25.
100. Roskoski, R., Jr., *RAF protein-serine/threonine kinases: structure and regulation*. *Biochem Biophys Res Commun*, 2010. **399**(3): p. 313-7.
101. Wartmann, M. and R.J. Davis, *The native structure of the activated Raf protein kinase is a membrane-bound multi-subunit complex*. *J Biol Chem*, 1994. **269**(9): p. 6695-701.
102. Wan, P.T., et al., *Mechanism of activation of the RAF-ERK signaling pathway by oncogenic mutations of B-RAF*. *Cell*, 2004. **116**(6): p. 855-67.
103. Sithanandam, G., et al., *B-raf and a B-raf pseudogene are located on 7q in man*. *Oncogene*, 1992. **7**(4): p. 795-9.

104. Williams, N.G. and T.M. Roberts, *Signal transduction pathways involving the Raf proto-oncogene*. *Cancer Metastasis Rev*, 1994. **13**(1): p. 105-16.
105. Davies, H., et al., *Mutations of the BRAF gene in human cancer*. *Nature*, 2002. **417**(6892): p. 949-54.
106. Cohen, Y., et al., *BRAF mutation in papillary thyroid carcinoma*. *J Natl Cancer Inst*, 2003. **95**(8): p. 625-7.
107. Kimura, E.T., et al., *High prevalence of BRAF mutations in thyroid cancer: genetic evidence for constitutive activation of the RET/PTC-RAS-BRAF signaling pathway in papillary thyroid carcinoma*. *Cancer Res*, 2003. **63**(7): p. 1454-7.
108. Garnett, M.J. and R. Marais, *Guilty as charged: B-RAF is a human oncogene*. *Cancer Cell*, 2004. **6**(4): p. 313-9.
109. Frattini, M., et al., *Alternative mutations of BRAF, RET and NTRK1 are associated with similar but distinct gene expression patterns in papillary thyroid cancer*. *Oncogene*, 2004. **23**(44): p. 7436-40.
110. Ciampi, R. and Y.E. Nikiforov, *Alterations of the BRAF gene in thyroid tumors*. *Endocr Pathol*, 2005. **16**(3): p. 163-72.
111. Xing, M., *BRAF mutation in thyroid cancer*. *Endocr Relat Cancer*, 2005. **12**(2): p. 245-62.
112. Nikiforova, M.N., et al., *BRAF mutations in thyroid tumors are restricted to papillary carcinomas and anaplastic or poorly differentiated carcinomas arising from papillary carcinomas*. *J Clin Endocrinol Metab*, 2003. **88**(11): p. 5399-404.
113. Liu, Z., et al., *A comparison of the clinicopathological features and prognoses of the classical and the tall cell variant of papillary thyroid cancer: a meta-analysis*. *Oncotarget*, 2017. **8**(4): p. 6222-6232.
114. Afkhami, M., et al., *Histopathologic and Clinical Characterization of Thyroid Tumors Carrying the BRAF(K601E) Mutation*. *Thyroid*, 2016. **26**(2): p. 242-7.
115. Torregrossa, L., et al., *Papillary Thyroid Carcinoma With Rare Exon 15 BRAF Mutation Has Indolent Behavior: A Single-Institution Experience*. *J Clin Endocrinol Metab*, 2016. **101**(11): p. 4413-4420.
116. Guerra, A., et al., *Genetic mutations in the treatment of anaplastic thyroid cancer: a systematic review*. *BMC Surg*, 2013. **13 Suppl 2**: p. S44.
117. Elisei, R., et al., *BRAF(V600E) mutation and outcome of patients with papillary thyroid carcinoma: a 15-year median follow-up study*. *J Clin Endocrinol Metab*, 2008. **93**(10): p. 3943-9.
118. Xing, M., et al., *BRAF mutation predicts a poorer clinical prognosis for papillary thyroid cancer*. *J Clin Endocrinol Metab*, 2005. **90**(12): p. 6373-9.
119. Elisei, R., et al., *The BRAF(V600E) mutation is an independent, poor prognostic factor for the outcome of patients with low-risk intrathyroid papillary thyroid carcinoma: single-institution results from a large cohort study*. *J Clin Endocrinol Metab*, 2012. **97**(12): p. 4390-8.
120. Trovisco, V., et al., *Type and prevalence of BRAF mutations are closely associated with papillary thyroid carcinoma histotype and patients' age but not with tumour aggressiveness*. *Virchows Arch*, 2005. **446**(6): p. 589-95.
121. Ito, Y., et al., *BRAF mutation in papillary thyroid carcinoma in a Japanese population: its lack of correlation with high-risk clinicopathological features and disease-free survival of patients*. *Endocr J*, 2009. **56**(1): p. 89-97.
122. Sancisi, V., et al., *BRAFV600E mutation does not mean distant metastasis in thyroid papillary carcinomas*. *J Clin Endocrinol Metab*, 2012. **97**(9): p. E1745-9.

123. Falchook, G.S., et al., *BRAF inhibitor dabrafenib in patients with metastatic BRAF-mutant thyroid cancer*. *Thyroid*, 2015. **25**(1): p. 71-7.
124. Nikiforov, Y.E., *Molecular diagnostics of thyroid tumors*. *Arch Pathol Lab Med*, 2011. **135**(5): p. 569-77.
125. Trovisco, V., et al., *BRAF mutations are associated with some histological types of papillary thyroid carcinoma*. *J Pathol*, 2004. **202**(2): p. 247-51.
126. Ciampi, R., et al., *Oncogenic AKAP9-BRAF fusion is a novel mechanism of MAPK pathway activation in thyroid cancer*. *J Clin Invest*, 2005. **115**(1): p. 94-101.
127. Yoshihara, K., et al., *The landscape and therapeutic relevance of cancer-associated transcript fusions*. *Oncogene*, 2015. **34**(37): p. 4845-54.
128. Kasaian, K., et al., *The genomic and transcriptomic landscape of anaplastic thyroid cancer: implications for therapy*. *BMC Cancer*, 2015. **15**: p. 984.
129. Yoo, S.K., et al., *Comprehensive Analysis of the Transcriptional and Mutational Landscape of Follicular and Papillary Thyroid Cancers*. *PLoS Genet*, 2016. **12**(8): p. e1006239.
130. Rajalingam, K., et al., *Ras oncogenes and their downstream targets*. *Biochim Biophys Acta*, 2007. **1773**(8): p. 1177-95.
131. Kanwar, M. and R.A. Kowluru, *Diabetes regulates small molecular weight G-protein, H-Ras, in the microvasculature of the retina: implication in the development of retinopathy*. *Microvasc Res*, 2008. **76**(3): p. 189-93.
132. Rapoport, M.J., et al., *Prevention of autoimmune diabetes by linomide in nonobese diabetic (NOD) mice is associated with up-regulation of the TCR-mediated activation of p21(ras)*. *J Immunol*, 1996. **157**(10): p. 4721-5.
133. Draznin, B., et al., *Effects of insulin on prenylation as a mechanism of potentially detrimental influence of hyperinsulinemia*. *Endocrinology*, 2000. **141**(4): p. 1310-6.
134. Kocher, H.M., et al., *Expression of Ras GTPases in normal kidney and in glomerulonephritis*. *Nephrol Dial Transplant*, 2003. **18**(11): p. 2284-92.
135. Rochefort, P., et al., *Thyroid pathologies in transgenic mice expressing a human activated Ras gene driven by a thyroglobulin promoter*. *Oncogene*, 1996. **12**(1): p. 111-8.
136. Vitagliano, D., et al., *Thyroid targeting of the N-ras(Gln61Lys) oncogene in transgenic mice results in follicular tumors that progress to poorly differentiated carcinomas*. *Oncogene*, 2006. **25**(39): p. 5467-74.
137. Forbes, S.A., et al., *COSMIC: mining complete cancer genomes in the Catalogue of Somatic Mutations in Cancer*. *Nucleic Acids Res*, 2011. **39**(Database issue): p. D945-50.
138. Vasko, V., et al., *Specific pattern of RAS oncogene mutations in follicular thyroid tumors*. *J Clin Endocrinol Metab*, 2003. **88**(6): p. 2745-52.
139. Basolo, F., et al., *N-ras mutation in poorly differentiated thyroid carcinomas: correlation with bone metastases and inverse correlation to thyroglobulin expression*. *Thyroid*, 2000. **10**(1): p. 19-23.
140. Garcia-Rostan, G., et al., *ras mutations are associated with aggressive tumor phenotypes and poor prognosis in thyroid cancer*. *J Clin Oncol*, 2003. **21**(17): p. 3226-35.
141. Volante, M., et al., *RAS mutations are the predominant molecular alteration in poorly differentiated thyroid carcinomas and bear prognostic impact*. *J Clin Endocrinol Metab*, 2009. **94**(12): p. 4735-41.
142. Moura, M.M., et al., *High prevalence of RAS mutations in RET-negative sporadic medullary thyroid carcinomas*. *J Clin Endocrinol Metab*, 2011. **96**(5): p. E863-8.

143. Boichard, A., et al., *Somatic RAS mutations occur in a large proportion of sporadic RET-negative medullary thyroid carcinomas and extend to a previously unidentified exon*. J Clin Endocrinol Metab, 2012. **97**(10): p. E2031-5.
144. Ciampi, R., et al., *Evidence of a low prevalence of RAS mutations in a large medullary thyroid cancer series*. Thyroid, 2013. **23**(1): p. 50-7.
145. Sheppard, K., et al., *Targeting PI3 kinase/AKT/mTOR signaling in cancer*. Crit Rev Oncog, 2012. **17**(1): p. 69-95.
146. Okumura, N., et al., *PI3K/AKT/PTEN Signaling as a Molecular Target in Leukemia Angiogenesis*. Adv Hematol, 2012. **2012**: p. 843085.
147. Cantley, L.C. and B.G. Neel, *New insights into tumor suppression: PTEN suppresses tumor formation by restraining the phosphoinositide 3-kinase/AKT pathway*. Proc Natl Acad Sci U S A, 1999. **96**(8): p. 4240-5.
148. Cully, M., et al., *Beyond PTEN mutations: the PI3K pathway as an integrator of multiple inputs during tumorigenesis*. Nat Rev Cancer, 2006. **6**(3): p. 184-92.
149. Fruman, D.A., R.E. Meyers, and L.C. Cantley, *Phosphoinositide kinases*. Annu Rev Biochem, 1998. **67**: p. 481-507.
150. Hers, I., E.E. Vincent, and J.M. Tavaré, *Akt signalling in health and disease*. Cell Signal, 2011. **23**(10): p. 1515-27.
151. Ringel, M.D., et al., *Overexpression and overactivation of Akt in thyroid carcinoma*. Cancer Res, 2001. **61**(16): p. 6105-11.
152. Engelman, J.A., J. Luo, and L.C. Cantley, *The evolution of phosphatidylinositol 3-kinases as regulators of growth and metabolism*. Nat Rev Genet, 2006. **7**(8): p. 606-19.
153. Chan, T.O. and P.N. Tsichlis, *PDK2: a complex tail in one Akt*. Sci STKE, 2001. **2001**(66): p. pe1.
154. Kwiatkowski, D.J., *Rhebbling up mTOR: new insights on TSC1 and TSC2, and the pathogenesis of tuberous sclerosis*. Cancer Biol Ther, 2003. **2**(5): p. 471-6.
155. Song, M.S., L. Salmena, and P.P. Pandolfi, *The functions and regulation of the PTEN tumour suppressor*. Nat Rev Mol Cell Biol, 2012. **13**(5): p. 283-96.
156. Liu, Z., et al., *Highly prevalent genetic alterations in receptor tyrosine kinases and phosphatidylinositol 3-kinase/akt and mitogen-activated protein kinase pathways in anaplastic and follicular thyroid cancers*. J Clin Endocrinol Metab, 2008. **93**(8): p. 3106-16.
157. Paes, J.E. and M.D. Ringel, *Dysregulation of the phosphatidylinositol 3-kinase pathway in thyroid neoplasia*. Endocrinol Metab Clin North Am, 2008. **37**(2): p. 375-87, viii-ix.
158. Santaripa, L., et al., *Phosphatidylinositol 3-kinase/akt and ras/raf-mitogen-activated protein kinase pathway mutations in anaplastic thyroid cancer*. J Clin Endocrinol Metab, 2008. **93**(1): p. 278-84.
159. Garcia-Rostan, G., et al., *Mutation of the PIK3CA gene in anaplastic thyroid cancer*. Cancer Res, 2005. **65**(22): p. 10199-207.
160. Ricarte-Filho, J.C., et al., *Mutational profile of advanced primary and metastatic radioactive iodine-refractory thyroid cancers reveals distinct pathogenetic roles for BRAF, PIK3CA, and AKT1*. Cancer Res, 2009. **69**(11): p. 4885-93.
161. Bruni, P., et al., *PTEN expression is reduced in a subset of sporadic thyroid carcinomas: evidence that PTEN-growth suppressing activity in thyroid cancer cells mediated by p27kip1*. Oncogene, 2000. **19**(28): p. 3146-55.

162. Gimm, O., et al., *Differential nuclear and cytoplasmic expression of PTEN in normal thyroid tissue, and benign and malignant epithelial thyroid tumors*. Am J Pathol, 2000. **156**(5): p. 1693-700.
163. Alvarez-Nunez, F., et al., *PTEN promoter methylation in sporadic thyroid carcinomas*. Thyroid, 2006. **16**(1): p. 17-23.
164. Hou, P., M. Ji, and M. Xing, *Association of PTEN gene methylation with genetic alterations in the phosphatidylinositol 3-kinase/AKT signaling pathway in thyroid tumors*. Cancer, 2008. **113**(9): p. 2440-7.
165. Liaw, D., et al., *Germline mutations of the PTEN gene in Cowden disease, an inherited breast and thyroid cancer syndrome*. Nat Genet, 1997. **16**(1): p. 64-7.
166. Rosen, E.D., et al., *PPAR gamma is required for the differentiation of adipose tissue in vivo and in vitro*. Mol Cell, 1999. **4**(4): p. 611-7.
167. Yamauchi, T., et al., *The mechanisms by which both heterozygous peroxisome proliferator-activated receptor gamma (PPARgamma) deficiency and PPARgamma agonist improve insulin resistance*. J Biol Chem, 2001. **276**(44): p. 41245-54.
168. McIver, B., S.K. Grebe, and N.L. Eberhardt, *The PAX8/PPAR gamma fusion oncogene as a potential therapeutic target in follicular thyroid carcinoma*. Curr Drug Targets Immune Endocr Metabol Disord, 2004. **4**(3): p. 221-34.
169. Eberhardt, N.L., et al., *The role of the PAX8/PPARgamma fusion oncogene in the pathogenesis of follicular thyroid cancer*. Mol Cell Endocrinol, 2010. **321**(1): p. 50-6.
170. Pasca di Magliano, M., R. Di Lauro, and M. Zannini, *Pax8 has a key role in thyroid cell differentiation*. Proc Natl Acad Sci U S A, 2000. **97**(24): p. 13144-9.
171. Raman, P. and R.J. Koenig, *Pax-8-PPAR-gamma fusion protein in thyroid carcinoma*. Nat Rev Endocrinol, 2014. **10**(10): p. 616-23.
172. Kroll, T.G., et al., *PAX8-PPARgamma1 fusion oncogene in human thyroid carcinoma [corrected]*. Science, 2000. **289**(5483): p. 1357-60.
173. Mascia, A., et al., *Hormonal control of the transcription factor Pax8 and its role in the regulation of thyroglobulin gene expression in thyroid cells*. J Endocrinol, 2002. **172**(1): p. 163-76.
174. Kondo, S., et al., *BBF2H7, a novel transmembrane bZIP transcription factor, is a new type of endoplasmic reticulum stress transducer*. Mol Cell Biol, 2007. **27**(5): p. 1716-29.
175. Nikiforova, M.N., et al., *RAS point mutations and PAX8-PPAR gamma rearrangement in thyroid tumors: evidence for distinct molecular pathways in thyroid follicular carcinoma*. J Clin Endocrinol Metab, 2003. **88**(5): p. 2318-26.
176. Sahin, M., et al., *PPARgamma staining as a surrogate for PAX8/PPARgamma fusion oncogene expression in follicular neoplasms: clinicopathological correlation and histopathological diagnostic value*. J Clin Endocrinol Metab, 2005. **90**(1): p. 463-8.
177. Castro, P., et al., *PAX8-PPARgamma rearrangement is frequently detected in the follicular variant of papillary thyroid carcinoma*. J Clin Endocrinol Metab, 2006. **91**(1): p. 213-20.
178. Jang, E.K., et al., *NRAS codon 61 mutation is associated with distant metastasis in patients with follicular thyroid carcinoma*. Thyroid, 2014. **24**(8): p. 1275-81.
179. Wang, H.M., et al., *Anaplastic carcinoma of the thyroid arising more often from follicular carcinoma than papillary carcinoma*. Ann Surg Oncol, 2007. **14**(10): p. 3011-8.

180. Fellegara, G. and J. Rosai, *Multifocal fibrosing thyroiditis: report of 55 cases of a poorly recognized entity*. Am J Surg Pathol, 2015. **39**(3): p. 416-24.
181. Batsakis, J.G., R.H. Nishiyama, and C.R. Rich, *Microlithiasis (calcospherites) and carcinoma of the thyroid gland*. Arch Pathol, 1960. **69**: p. 493-8.
182. Johannessen, J.V. and M. Sobrinho-Simoes, *The origin and significance of thyroid psammoma bodies*. Lab Invest, 1980. **43**(3): p. 287-96.
183. Klinck, G.H. and T. Winship, *Psammoma bodies and thyroid cancer*. Cancer, 1959. **12**(4): p. 656-62.
184. Yao, Z., et al., *Tumours with class 3 BRAF mutants are sensitive to the inhibition of activated RAS*. Nature, 2017. **548**(7666): p. 234-238.
185. Cameselle-Teijeiro, J., et al., *BRAF mutation in solid cell nest hyperplasia associated with papillary thyroid carcinoma. A precursor lesion?* Hum Pathol, 2009. **40**(7): p. 1029-35.
186. Tschandl, P., et al., *NRAS and BRAF mutations in melanoma-associated nevi and uninvolved nevi*. PLoS One, 2013. **8**(7): p. e69639.
187. Gaiser, M.R., et al., *Variables that influence BRAF mutation probability: A next-generation sequencing, non-interventional investigation of BRAFV600 mutation status in melanoma*. PLoS One, 2017. **12**(11): p. e0188602.
188. Kinno, T., et al., *Clinicopathological features of nonsmall cell lung carcinomas with BRAF mutations*. Ann Oncol, 2014. **25**(1): p. 138-42.
189. Rebocho, A.P. and R. Marais, *ARAF acts as a scaffold to stabilize BRAF:CRAF heterodimers*. Oncogene, 2013. **32**(26): p. 3207-12.
190. Mitmaker, E., et al., *Microsatellite instability in benign and malignant thyroid neoplasms*. J Surg Res, 2008. **150**(1): p. 40-8.
191. Nikiforov, Y.E., M. Nikiforova, and J.A. Fagin, *Prevalence of minisatellite and microsatellite instability in radiation-induced post-Chernobyl pediatric thyroid carcinomas*. Oncogene, 1998. **17**(15): p. 1983-8.

Supplementary Table 1: Genes included in our RNA-based expression pannel

Gene	Breakpoints	Annotation	Detail
AGK-/-BRAF	1	PTC	Gene Fusion
AKAP13-/-RET	1	PTC	Gene Fusion
AKAP9-/-BRAF	2	PTC	Gene Fusion
CCDC6-/-RET	3	PTC	Gene Fusion
CREB3L2-/-PPARG	1	FC	Gene Fusion
EML4-/-ALK	36	PTC	Gene Fusion
ERC1-/-RET	7	PTC	Gene Fusion
ETV6-/-NTRK3	2	PTC	Gene Fusion
FGFR2-/-OFD1	1	PTC	Gene Fusion
GOLGA5_PTC5-/-RET	1	PTC	Gene Fusion
HOOK3-/-RET	1	PTC	Gene Fusion
KTN1-/-RET	1	PTC	Gene Fusion
MACF1-/-BRAF	1	PTC	Gene Fusion
MKRN1-/-BRAF	1	PTC	Gene Fusion

NTRK1-/-TFG	6	PTC	Gene Fusion
NTRK3-/-ETV6	1	PTC	Gene Fusion
PAX8-/-PPARG	5	FC	Gene Fusion
PCM1-/-RET	2	PTC	Gene Fusion
PRKAR1A-/-RET	2	PTC	Gene Fusion
RET-/-TRIM33	1	PTC	Gene Fusion
SND1-/-BRAF	1	PTC	Gene Fusion
SQSTM1-/-NTRK1	1	PTC	Gene Fusion
SSBP2-/-NTRK1	1	PTC	Gene Fusion
TBL1XR1-/-RET	2	PTC	Gene Fusion
TFG-/-ALK	3	PTC	Gene Fusion
TPM3-/-NTRK1	1	PTC	Gene Fusion
TPR-/-NTRK1	1	PTC	Gene Fusion
TRIM24-/-RET	3	PTC	Gene Fusion
TRIM27-/-RET	2	PTC	Gene Fusion

TRIM33-/-RET	2	PTC	Gene Fusion
CITED1	-	Biomarker	Gene Expression
KLK10	-	Biomarker	Gene Expression
FHL1	-	BRAF down	Gene Expression
HLF	-	BRAF down	Gene Expression
IRS1	-	BRAF down	Gene Expression
MMP15	-	BRAF down	Gene Expression
TFF3	-	BRAF down	Gene Expression
ANXA1	-	BRAF signature	Gene Expression
DUSP5	-	BRAF signature	Gene Expression
PROS1	-	BRAF signature	Gene Expression
SDC4	-	BRAF signature	Gene Expression
SLC35F2	-	BRAF signature	Gene Expression
SYT12	-	BRAF signature	Gene Expression
ARNTL	-	BRAF signature BRAF up	Gene Expression

FN1	-	BRAF signature BRAF up	Gene Expression
MET	-	BRAF signature Expressed fusion	Gene Expression
DCSTAMP	-	BRAF up	Gene Expression
ERBB3	-	BRAF up	Gene Expression
GATA3	-	BRAF up	Gene Expression
GNLY	-	BRAF up	Gene Expression
ITGB6	-	BRAF up	Gene Expression
TMPRSS6	-	BRAF up	Gene Expression
TPD52L1	-	BRAF up	Gene Expression
SFTPB	-	BRAF/RET up	Gene Expression
IPCEF1	-	Cancer down	Gene Expression
PAPSS2	-	Cancer down	Gene Expression
RGS16	-	Cancer down	Gene Expression
ENTPD1	-	Cancer up	Gene Expression
LRP4	-	Cancer up	Gene Expression

ALK	-	Expressed fusion	Gene Expression
BRAF	-	Expressed fusion	Gene Expression
FGFR2	-	Expressed fusion	Gene Expression
NTRK1	-	Expressed fusion	Gene Expression
NTRK3	-	Expressed fusion	Gene Expression
PPARG	-	Expressed fusion	Gene Expression
RAF1	-	Expressed fusion	Gene Expression
ROS1	-	Expressed fusion	Gene Expression
THADA	-	Expressed fusion	Gene Expression
AAMP	-	Housekeeping	Gene Expression
AAR2	-	Housekeeping	Gene Expression
ACTB	-	Housekeeping	Gene Expression
ARF1	-	Housekeeping	Gene Expression
ATP5E	-	Housekeeping	Gene Expression
CLTC	-	Housekeeping	Gene Expression

DEDD	-	Housekeeping	Gene Expression
GAPDH	-	Housekeeping	Gene Expression
GPKOW	-	Housekeeping	Gene Expression
GPS1	-	Housekeeping	Gene Expression
GPX1	-	Housekeeping	Gene Expression
HMBS	-	Housekeeping	Gene Expression
MMADHC	-	Housekeeping	Gene Expression
MRFAP1	-	Housekeeping	Gene Expression
MRPS9	-	Housekeeping	Gene Expression
PGK1	-	Housekeeping	Gene Expression
PPP2CA	-	Housekeeping	Gene Expression
PSMA1	-	Housekeeping	Gene Expression
PSMC1	-	Housekeeping	Gene Expression
RPL13A	-	Housekeeping	Gene Expression
RPL37	-	Housekeeping	Gene Expression

RPL8	-	Housekeeping	Gene Expression
SDHA	-	Housekeeping	Gene Expression
SLC25A3	-	Housekeeping	Gene Expression
TXNL1	-	Housekeeping	Gene Expression
UBA52	-	Housekeeping	Gene Expression
ZC3HC1	-	Housekeeping	Gene Expression
CD274	-	Immuno-oncology	Gene Expression
CD8A	-	Immuno-oncology	Gene Expression
CD8B	-	Immuno-oncology	Gene Expression
CTLA4	-	Immuno-oncology	Gene Expression
CXCL10	-	Immuno-oncology	Gene Expression
CXCL9	-	Immuno-oncology	Gene Expression
FOXP3	-	Immuno-oncology	Gene Expression
GZMA	-	Immuno-oncology	Gene Expression
HAVCR2	-	Immuno-oncology	Gene Expression

IDO1	-	Immuno-oncology	Gene Expression
LAG3	-	Immuno-oncology	Gene Expression
PDCD1	-	Immuno-oncology	Gene Expression
PDCD1LG2	-	Immuno-oncology	Gene Expression
PRF1	-	Immuno-oncology	Gene Expression
TIGIT	-	Immuno-oncology	Gene Expression
TMEM173	-	Immuno-oncology	Gene Expression
TNFRSF4	-	Immuno-oncology	Gene Expression
TNFRSF9	-	Immuno-oncology	Gene Expression
CALCA	-	Lineage	Gene Expression
CEACAM5	-	Lineage	Gene Expression
CGA	-	Lineage	Gene Expression
PAX8	-	Lineage	Gene Expression
TP63	-	Lineage	Gene Expression
TTF1	-	Lineage	Gene Expression

ASF1B	-	Proliferation	Gene Expression
ASPM	-	Proliferation	Gene Expression
AURKA	-	Proliferation	Gene Expression
BIRC5	-	Proliferation	Gene Expression
BUB1B	-	Proliferation	Gene Expression
CDC20	-	Proliferation	Gene Expression
CDCA3	-	Proliferation	Gene Expression
CDCA8	-	Proliferation	Gene Expression
CDK1	-	Proliferation	Gene Expression
CDK4	-	Proliferation	Gene Expression
CDKN3	-	Proliferation	Gene Expression
CENPF	-	Proliferation	Gene Expression
CENPM	-	Proliferation	Gene Expression
CEP55	-	Proliferation	Gene Expression
DLGAP5	-	Proliferation	Gene Expression

DTL	-	Proliferation	Gene Expression
EZH2	-	Proliferation	Gene Expression
FOXM1	-	Proliferation	Gene Expression
KIAA0101	-	Proliferation	Gene Expression
KIF11	-	Proliferation	Gene Expression
KIF20A	-	Proliferation	Gene Expression
MCM10	-	Proliferation	Gene Expression
MCM4	-	Proliferation	Gene Expression
MKI67	-	Proliferation	Gene Expression
NUSAP1	-	Proliferation	Gene Expression
ORC6	-	Proliferation	Gene Expression
PBK	-	Proliferation	Gene Expression
PLK1	-	Proliferation	Gene Expression
PRC1	-	Proliferation	Gene Expression
PTTG1	-	Proliferation	Gene Expression

RAD51	-	Proliferation	Gene Expression
RAD54L	-	Proliferation	Gene Expression
RRM2	-	Proliferation	Gene Expression
SKA1	-	Proliferation	Gene Expression
TK1	-	Proliferation	Gene Expression
TOP2A	-	Proliferation	Gene Expression
TPX2	-	Proliferation	Gene Expression
UBE2C	-	Proliferation	Gene Expression
CFH	-	RAS down	Gene Expression
S100A10	-	RAS down	Gene Expression
ANKRD46	-	RAS signature	Gene Expression
CYB561	-	RAS signature	Gene Expression
GNA14	-	RAS signature	Gene Expression
KATNAL2	-	RAS signature	Gene Expression
LGI3	-	RAS signature	Gene Expression

MLEC	-	RAS signature	Gene Expression
SFTPC	-	RAS signature	Gene Expression
HGD	-	RAS signature BRAF down	Gene Expression
SORBS2	-	RAS signature BRAF down	Gene Expression
KCNAB1	-	RAS signature RAS up	Gene Expression
NQO1	-	RAS signature RAS up	Gene Expression
SLC4A4	-	RAS signature RAS up	Gene Expression
PIWIL1	-	RAS up	Gene Expression
SNRNP25	-	RAS up	Gene Expression
MBNL2	-	RET down	Gene Expression
MYL4	-	RET up	Gene Expression
SORBS1	-	RET up	Gene Expression
TNXB	-	RET up	Gene Expression
DIO2	-	Thyroid differentiation score	Gene Expression
DUOX1	-	Thyroid differentiation score	Gene Expression

DUOX2	-	Thyroid differentiation score	Gene Expression
SLC26A4	-	Thyroid differentiation score	Gene Expression
SLC5A8	-	Thyroid differentiation score	Gene Expression
TG	-	Thyroid differentiation score	Gene Expression
TPO	-	Thyroid differentiation score	Gene Expression
DIO1	-	Thyroid differentiation score RAS up	Gene Expression